ExoStride

An Assistive Knee Exoskeleton

ME 47300, ME 47400

Senior Design

Ben Bokser

Michael Sidoo

Richard Wilson

Valentine Adesman

Diego Monastra

Brian Lui

Professor: Ali Sadegh

Contents

Abstract

An assistive knee exoskeleton is designed, manufactured and tested to reduce metabolic cost in lifting applications. Overexertion in lifting is a common cause of knee and back injuries, and the chance of such injuries occurring can be mitigated with the use of augmentations. A cable drive is used to create a novel exoskeleton design that is simultaneously flexible, powerful and lightweight with less distal inertia than previous works. Three main iterations of the prototype are manufactured; the final one reinforced with carbon fiber. Finite Element Analysis is used to validate aluminum components and physical testing of the motor is considered. The final prototype is demonstrably comfortable, lightweight, and actuates in unison with human joint movement.

1. Introduction

1.1. Project Description

This report details the process undertaken for our senior design project. After an exhaustive literature review and patent search, the design concept was developed. A thorough solid model was designed using a combination of 3D-printed and off-the-shelf (OTS) parts. This design was iteratively developed and changed considerably over the process of prototyping, although the overall concept remained the same. Three main iterations of the prototype were manufactured; the final one reinforced with carbon fiber. Finite Element Analysis was used to validate aluminum components. Through an iterative process, we eventually reached a working prototype that fulfilled all requirements.

Task Name	Duration	Start	Finish	Predecessors
Select Project	1 wk	Thu 8/31/17	Wed 9/6/17	
Choose between Passive or Active System	2 wks	Thu 9/7/17	Wed 9/20/17	1
Select method of actuation	3 wks	Thu 9/21/17	Wed 10/11/1	2
Test Proof of Concept	1 wk	Thu 10/12/17	Wed 10/18/1	3
Create solid model of exoskeleton	4 wks	Thu 10/19/17	Wed 11/15/1	4
Manufacture an Alpha protoype	4 wks	Thu 11/16/17	Wed 12/13/1	5
Redesign alpha prototype	6.6 wks	Thu 12/14/17	Sat 1/27/18	6
Select Sensors that will be used for user intention	1 wk	Mon 1/29/18	Fri 2/2/18	7
Purchase Sensor	1 wk	Mon 2/5/18	Fri 2/9/18	8
Design Electrical Systems	4 wks	Mon 2/5/18	Fri 3/2/18	8
Purchase Electronics	2 wks	Mon 3/5/18	Fri 3/16/18	10
Test Electronics using basic	3 wks	Mon 3/19/18	Fri 4/6/18	11
Intergrate Electronics into Exoskeleton	2 wks	Mon 4/9/18	Fri 4/20/18	12
Write Code for IMU to collect Data	4 wks	Mon 2/5/18	Fri 3/2/18	8
Intergrate IMU into Control Algorithm	4 wks	Mon 3/5/18	Fri 3/30/18	14
Intergrate Control Algorithm into electronics	3 wks	Mon 4/2/18	Fri 4/20/18	15
Develop method to manufacture the different parts	3 wks	Mon 2/5/18	Fri 2/23/18	8
3D print the beta prototype	3 wks	Mon 2/26/18	Fri 3/16/18	17
Layer the 3D parts in carbon fiber	5 wks	Mon 3/19/18	Fri 4/20/18	18
Intergrate all the component together	2 wks	Mon 4/23/18	Fri 5/4/18	19,16,13

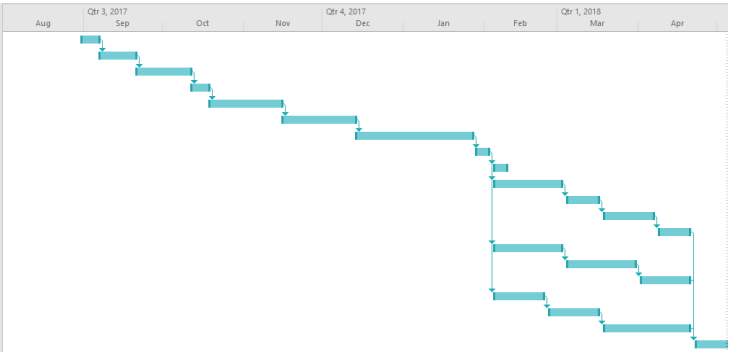

Figure 1. Gantt Chart used to schedule the development process.

1.2. Motivation

Our original senior design assignment was to develop a knee augmentation for the army, with the goal to help soldiers support more weight while carrying heavier loads and to reduce the possibility of knee related injuries. Unfortunately, the project was almost immediately canceled by the original sponsor. With no sponsor, our project lacked further direction. Fortunately, we had already entered the Zahn Competition due to Professor Sadegh's recommendation. We had adapted our design to provide aid to the civilian workforce, specifically those who perform repetitive actions that require lower body strength such as lifting. As such, we were able to easily transition the design requirement from helping soldiers to helping workers. Now, our goal is to help these workers by designing a knee augmentation device that will reduce the number of knee-related workplace injuries. From a business perspective, our device will also save corporations money by reducing the number of workers' compensation payouts due to knee injuries suffered in the workplace.

We will not settle on a prototype that simply worked; in order to make our design viable for consumer use, we will continuously test and improve our design iteratively until we are fully confident in it. As members of the newly founded ExoStride, we are not simply making a senior design project; instead, we are designing a product meant to improve and revolutionize an industry.

1.3. Problem Statement

According to the Bureau of Labor Statistics and the National Electronic Injury Surveillance System (Chen 2013), approximately 184,300 people are injured every year in knee-related injuries while at work. They defined an injury as an incident requiring more than two days off of work to recuperate (Chen 2013). This accounts for 5% of all work-related injuries. This is second only to back, which has a 15% rate of injury in the workplace (BLS, 2011). The most common cause of knee injuries is overexertion and sprains. Typically, these result in tearing of the muscles around the knee. This damage is frequently caused by "repetitive knee flexion and extension," which is an issue that our design will directly address. It was also determined that the average workers' compensation claim for a knee injury at the workplace was $20,222, and 49% of all claims involved greater than 3 days of lost work time (Chen 2013). This research informed us as to the prevalence of knee injuries in the workplace, as well as the economic cost of such injuries.

1.4. Background/Literature Review

In order to effectively fulfill our project requirements, we first conducted preliminary research. This included an exhaustive patent search, an investigation into currently existing exoskeletons, and research into the current existing literature regarding the knee-joint and exoskeletal assistance. The goal of the literature search was to be able to understand the

requirements that the user will need, to gain as much knowledge as possible, understand currently existing patents, and ensure that our idea will be superior to other existing ideas.

First, investigative research was conducted into the biology of the knee joint. To do this, textbooks pertaining to the biomechanics of the knee were researched (Pockock, 2013). One of the first revelations we had was the complexity of the knee joint. There are four bones that make up the knee joint: The tibia, the patella, the femur and the fibula. The tibia is colloquially called the shin bone and runs from the knee to the ankle. On top of the tibia on each side are two menisci, which help stabilize the knee. The patella is colloquially called the kneecap and is a small flat triangular bone that relieves friction between the other bones of the knee. The patella acts as a fulcrum to give the leg its power. The femur is colloquially called the thigh bone and is the largest, longest, strongest bone in the body. The fibula is the long, thin bone in the lower leg on the lateral side and runs next to the tibia from the knee to the ankle. There is also a collection of ligaments, which attach bones to bones for strength and stability, as well as tendons, which are part of the muscle, connecting muscles to bones. The two major muscle groups around the knee are the quadriceps, which are four muscles located in the thigh and straighten the knee, and the hamstrings, which move the leg from a straight to bent position.

The general purpose of the knee is to allow locomotion with minimal energy requirements from the surrounding muscles, to allow stability while traversing unsteady terrain, and to transmit, absorb, and distribute forces from walking, jumping and lifting (Hirokawa 1993). The knee joint has six degrees of freedom, three rotational degrees and three translational degrees. For rotation, the knee is capable of allowing for flexion up to 150 degrees with ~10 degrees of hyperextension. There is also 25-30 degrees of internal-external rotation. The primary translational motion is from anterior (front) to posterior (back); the knee joint is capable of sliding approximately 5-10mm. The knee joint can also translate in compression and laterally. These discoveries enlightened us as to the complex motions involved in the knee, and we decided we must try to keep as many of these degrees of freedom as possible.

Research was also conducted into analyzing the typical gait of a human. It was necessary for us to examine the gait of a typical human and compare that to the gait of a human wearing an exoskeleton. The gait of a human is separated in several steps: the stance phase, the stance phase reversal, the toe off, the swing phase, and initial contact (Perry, 1992). The toe off occurs at approximately 39% of the gait, and the initial contact marks the final completion of the step. We learned that the ideal point to implement the exoskeleton is right after the toe off face and into the swing phase. In studies, people who wore exoskeletons reached the peak of leg flexion during the swing phase much earlier than without an exoskeleton. The researchers speculated that this is because wearing an exoskeleton reduces the center of gravity of the user, causing them to achieve balance earlier. This is an important consideration for our design (Perry, 1992).

In an article by Tadej Petrič et. Al. published in Advance Robotics (Petrič T, 2013), the researchers specifically look at a knee exoskeleton designed to assist the user in continuously undergoing the squat motion. A user wore the exoskeleton while several monitoring devices were attached. These devices monitored heart rate, blood oxygen saturation, oxygen

consumption, ventilation, and electromyography (EMG) sensors. EMG sensors record and analyze the electrical activity of muscles during activation. The aim of the study was to evaluate three different control schemes for the exoskeleton. For our purposes, those control schemes were not immediately important to us, as we decided to save an examination of possible control schemes until much later in the development cycle. What was important, however, were the devices they used to monitor the human. When developing an exoskeleton, empirical evidence is required in order to demonstrate the effectiveness of its assistance. Simply stating that you can feel assistance is not enough, you must prove that the assistance is empirically significant. These sensors provided insight into the methods we could use to measure this. The study also concluded that an assistive exoskeleton was able to increase the torque of the knee in all control cases when compared to a human not wearing the exoskeleton. Additionally, the study found that for all control methods, the body kinematics of the human were greatly different than without the exoskeleton. This is likely due to restriction of motion and change of center of gravity. These are all necessary considerations for our design.

In addition to a literature review, we needed to conduct a patent search. Through the patent search, we began to explore the existing models of robotic knee exoskeletons. The goal of the patent search was to ensure that the design we come up with is relatively innovative, to ensure that our design has advantages that others do not, and to ensure that our design does not have the disadvantages that others do.

During our patent search, we discovered several existing knee exoskeletons. There are too many to discuss in this paper, so a few key designs will be chosen. The first existing design we discovered was the hybrid assistive limb (HAL) exoskeleton developed by Cyberdyne. This is a full body exoskeleton with emphasis on gait assistance and strength augmentation. Their most recent model is the HAL-5. This design uses localized motors to actuate the joints, while an onboard battery is placed on the back. The battery allows for 160 minutes of operation, and allows the exoskeleton to lift 70kg. The control system of the HAL-5 involves the use of EMG sensors to monitor and estimate muscle torque. The benefits of this system are that the level of augmentation provided is large, and the battery life is fairly long. The primary downsides are that the augmentation is bulky, and requires precise calibration to fit onto the user. If the dimensions of the user change, such as weight gain or loss, the suit must be recalibrated, which is a lengthy and expensive procedure.

Another existing model we decided to look at is the MIT Exoskeleton. This exoskeleton is a quasi-passive design which harnesses energy that is exchanged between gravity and inertia. This design combines active and passive elements. Springs, variable impedance joints and powered actuators are used. This exoskeleton is primarily designed to assist gait and also designed to allow the user to run longer distances. The primary mover is a series-elastic linear ball screw, which is extremely efficient at transferring loads and actuating the exoskeleton. The main benefits of this exoskeleton are that it is very lightweight, and was designed specifically not to interfere with the user's typical gait pattern. The primary disadvantages are that the battery life is low at only 30 minutes, and the exoskeleton is very heavy. These are scenarios that we will tackle during our design.

Another exoskeleton that we looked at is the Titan Arm. Although this is an arm exoskeleton, the design is relatable to knee augmentations. This augmentation uses a tetherless design that incorporates a battery and motor attached to the back. Through a cable drive, the motor is connected to the arm. By allowing the battery and motor to rest on the back rather than localizing them at the area of the joint, the exoskeleton becomes much more comfortable. This is because the back is better at carrying a distributed load than any joint is. The cable drive that the Titan Arm uses is innovative and effective to transmit forces. It allows the Titan Arm to augment the user's lifting strength by 40 lbs. We decided to use the cable drive of the Titan Arm as an inspiration for our knee augmentation.

2. Design Process

2.1. Concept

After reviewing the downsides and failures of existing technology, as well as conducting approximately 20 interviews with various warehouse workers, it was clear that our exoskeleton should be optimized for low weight, low cost, ease of control, minimum volume, high efficiency, and comfort. Quantitative and qualitative requirements determined are as follows: (1) the device should weigh no more than 6 kg or 13 lbs, (2) the device should provide a lifting power of approximately 40 Nm or 28% of peak human knee torque, (3) the device should be comfortable and convenient - it should not take up too much space and not hinder movement, (4) it should be possible to attach and remove the device within 3 minutes.

Based on these parameters, we were able to compare various methods of actuation, as tabulated in Figure 2 below.

	Geared DC Motor	Cable Drive	Flex Shaft	Pneumatic	Hydraulic	Shape Memory	Pneumatic Bag
Cost	Cheap	Cheap	Cheap	Medium	Expensive	Medium	Medium
Weight	Medium	Light	Light	Medium	Heavy	Light	Light
Power	Good	Good	Good	Medium	Powerful	Weak	Low
Efficiency	Good	Good	Medium	Medium	Medium	Inefficient	Low
Control	Easy	Easy	Easy	Difficult	Difficult	Easy	Medium
Size/Space	Large	Medium	Medium	Medium	Large	Small	Small
Comfort	Medium	Good	Medium	Good	Bad	Good	Good
Reliability	Good	Good	Good	Medium	Medium	Medium	Medium

Figure 2. Comparison of actuation and power transmission methods.

Following this evaluation of actuation methods, three top design concepts were developed, as shown below in Figure 3. The top three concepts were as follows; (1) the use of a planetary gearbox motor mounted directly at the knee joint, (2) the use of a cable drive with motor mounted at the hip, and (3) the use of a passive leaf spring to store potential energy. Other actuation methods, such as pneumatics and hydraulics, take up a considerable amount of space. They were also found to be overly massive, difficult to control, and expensive. On the other hand, methods such as shape memory alloy were found to be too weak and inefficient for the application.

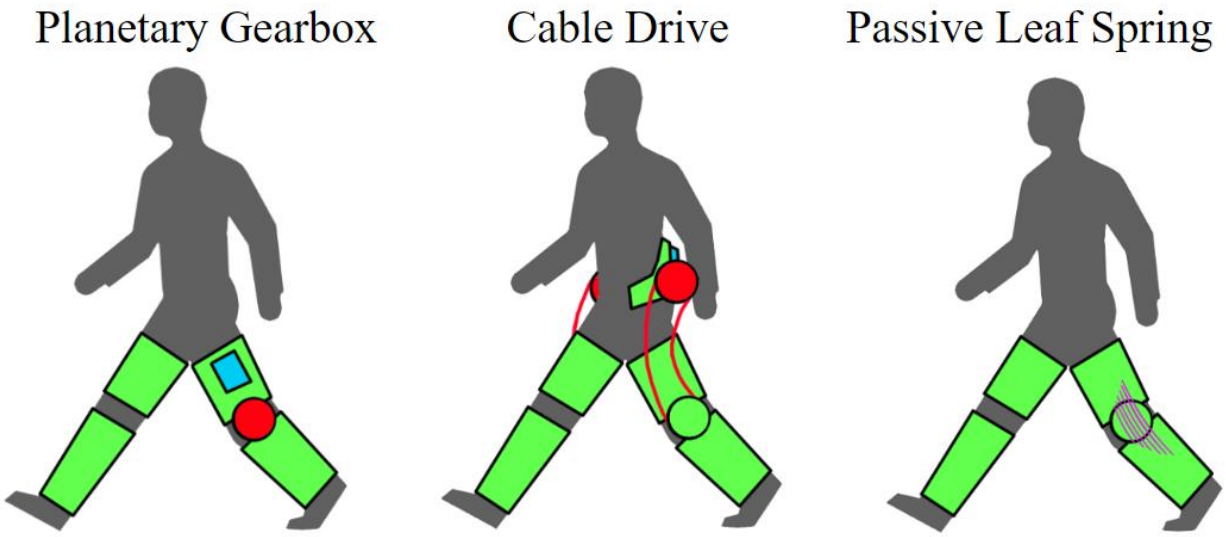

Figure 3. The top three design concepts.

As shown, the planetary gearbox concept scored lowest due to its size and weight issues despite its reliability. Using a geared DC motor drive by itself is very common in robotics. However, in the case of an exoskeleton, having the geared motor driving the knee joint would require the motor and gearbox to rest near the joint. This is sub-optimal for metabolic efficiency, as it forces the user to put more effort into every step by adding mass to the leg. It would also cause the profile of the exoskeleton to no longer be form-fitting, by adding a volume that extends out from the leg considerably.

While the leaf spring design was seriously considered, ultimately its lack of comfort, control and power prevented it from being the top pick. It is also not a very novel design, as medical knee braces already operate on similar concepts.

From this chart, it became obvious that the top concept was the cable drive as shown in Figure 5. The cable drive is a very lightweight form of power transmission similar to a belt drive; however, it is more flexible and adaptive than a belt drive.

Category	Weight of Category	Planetary Gearbox Drive	Cable Drive	Passive Leaf Spring
Cost	5	-1	+1	+1
Weight	20	0	+1	+1
Power	10	+1	+1	-1
Efficiency	10	+1	+1	+1
Control	5	+1	+1	0
Size	15	-1	0	+1
Comfort	15	0	+1	0
Reliability	20	+1	+1	+1
Total	100	+25	+85	+60

Figure 4. Evaluation of the top three concepts.

Our cable drive design allows for non-localized actuation. Instead of forcing the user to carry the weight of the motor and gearbox on the leg, which increases the amount of work done with each step, the motor and gearbox are positioned on the lower back – close to the center of gravity of the body. This is known as reduction of distal inertia. It also reduces the amount of space that the knee augmentation uses, making it more form-fitting. A cable housing and Bowden cable allow for a flexible power transmission that bends with the user's hip rotation, without a significant reduction in efficiency.

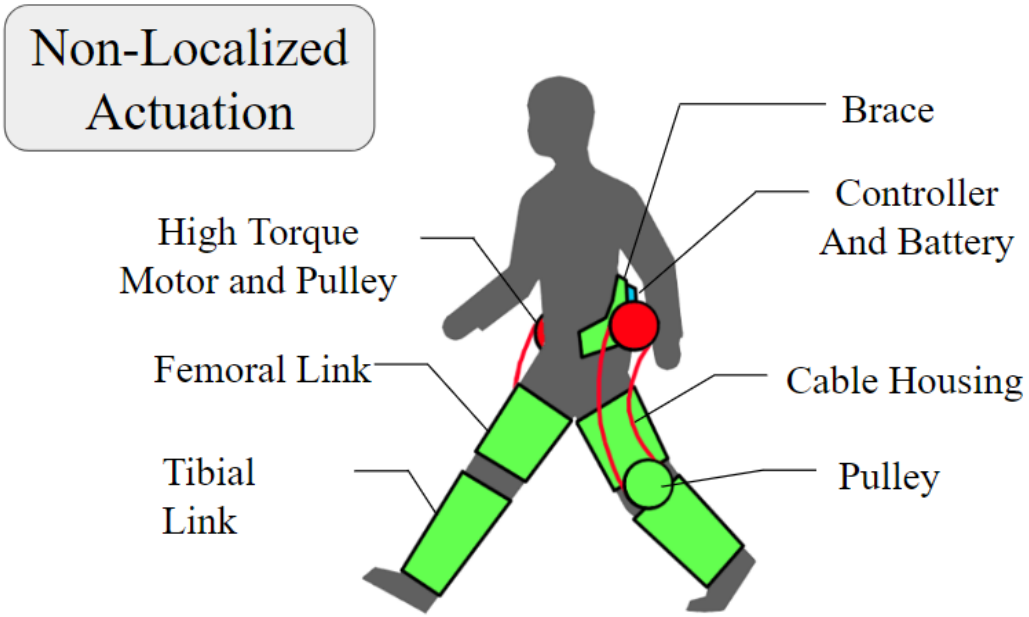

Figure 5. Detailed cable drive concept.

2.2. Design

2.2.1. The Initial Prototyping Phase

The first iteration of the knee augmentation was then modelled in Solidworks as shown in Figure 6. As shown, the pulleys are CNC milled from 6061-T6 aluminum stock. A lathe would also be used in order to create the grooves. A cable stop mount is screwed directly into a recess in the pulley. The purpose of the cable stop mount is to hold the cable stops, which prevent the cable from slipping out and allow transmission of cable tension into pulley torque. The knee joint rotates around a set of ball bearings. Crossbars, made of bent aluminum sheeting, hold the two sides of the assembly together.

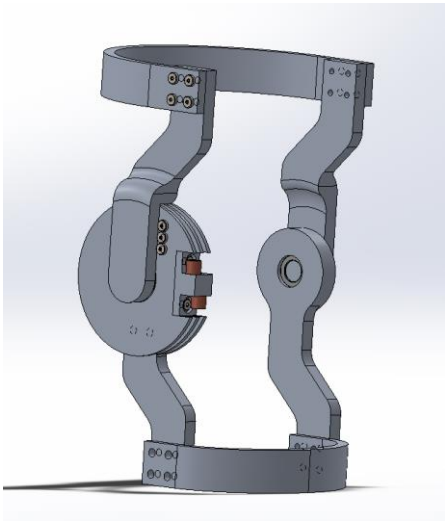

Figure 6. First iteration of the knee joint assembly.

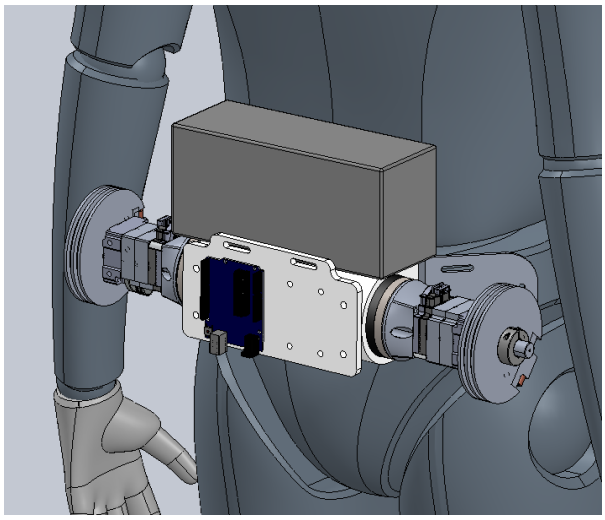

Figure 7. First iteration of the back brace assembly.

A nearly identical pulley was connected to the motor shaft. A 215-watt motor was used. Its gear ratio is 63:1. The output torque reached 44 Newton-meters at maximum power. Shown in Figure 8 is the first iteration of the back brace assembly, including the motors. The back brace holds all of the electronics – An Arduino motor controller and a 16 Amp-hour lithium polymer battery - other than the sensors. It is strapped around the user's waist, as well as over the user's shoulders.

After our first iteration of the knee augmentation design was modelled, we used 3D-printing to create a prototype (Figure 8).

Figure 8. The first prototype.

From this prototype, we were able to determine a large number of flaws in our first design. One major flaw lay in the placement of the straps. Strap slots had not been modelled yet, and so the straps slipped off easily. There was only enough space for one strap on each of the two members, meaning there were only two points of contact with the leg, as shown in Figure 9. When tested, the leg augmentation did not properly grip the leg in such a way as to rotate the knee joint. As such, it was determined that two points of contact for the entire leg was not enough. Instead, there should be two points of contact for each member of the leg, for a total of four points of contact – so four straps. In order to allow for the placement of four straps, the augmentation had to be made longer.

Additionally, there was difficulty in attaching the augmentation to the user's leg, as the crossbars were on opposite sides – meaning that the user had to slip his or her leg in between them. Instead, the crossbars needed to be moved to the same side. Shown in Figure 10 is the next model that was created as a result of prototype testing. In this model, the augmentation was made longer, four strap slots were created on each side, the crossbars were moved to the front, and additional cross bars were added.

Despite the flaws in the human-machine interface, a test of the actuation method proved successful. As shown in Figure 12, the actuation method was tested using a string as the cable. The pulley motor was controlled using a radio receiver. The exoskeleton was capable of extending and retracting in sync with user commands, even when the cable housing was bent to a 90 degree angle. This proved that the cable drive was feasible.

Figure 10. Wearing the first prototype.

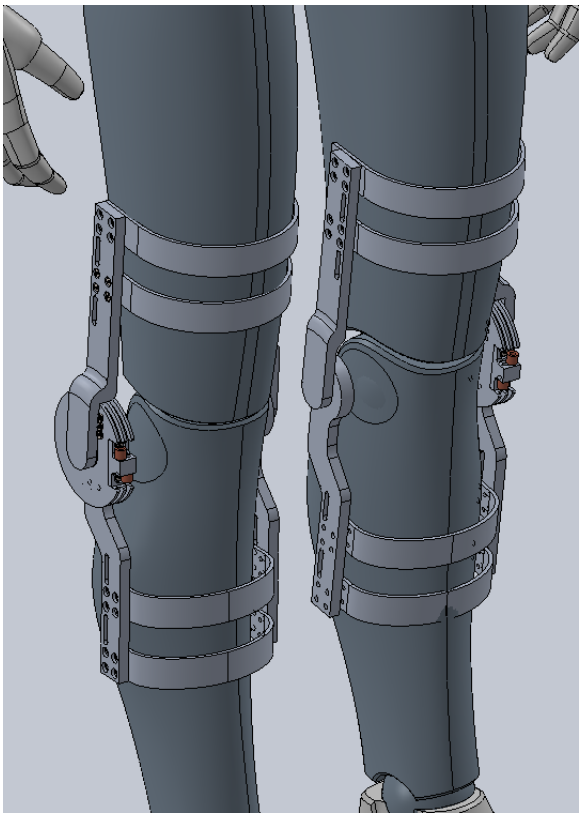

Figure 11. The resultant design changes.

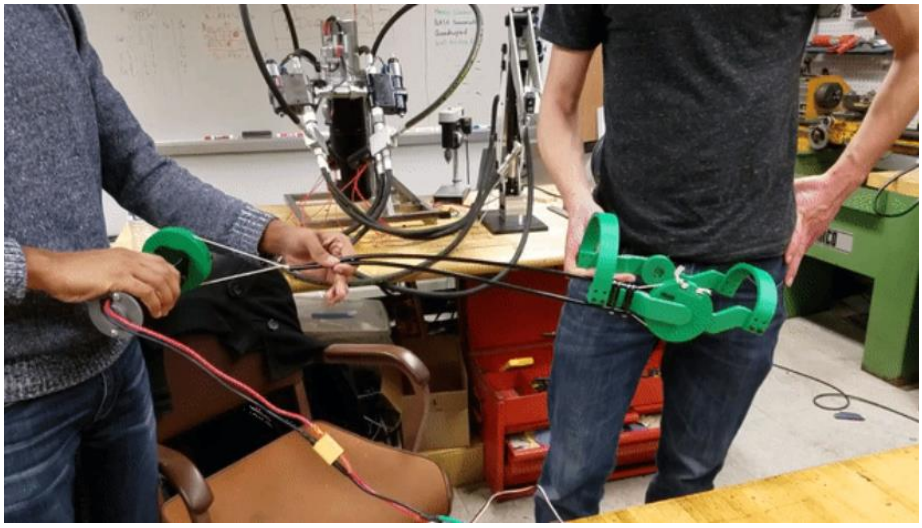

Figure 12. Actuation testing of the first prototype.

2.2.2. The Final Design

After careful deliberation, a large amount of changes were made to the design before moving onto further prototyping, without dramatically changing the overall concept. A high torque density BLDC pancake motor was provided by Professor Hao Su. This custom-made motor has a torque rating of up to 5 Newton meters. To reach the desired maximum torque of 40 Newton meters, a 1:8 gear ratio was chosen. But instead of using a gearbox, the pulley system was redesigned to inherently provide this required mechanical advantage.

Additionally, the design of the femoral and tibial links was greatly modified to be more lightweight, comfortable and form-fitting, as shown in Figure 13 below.

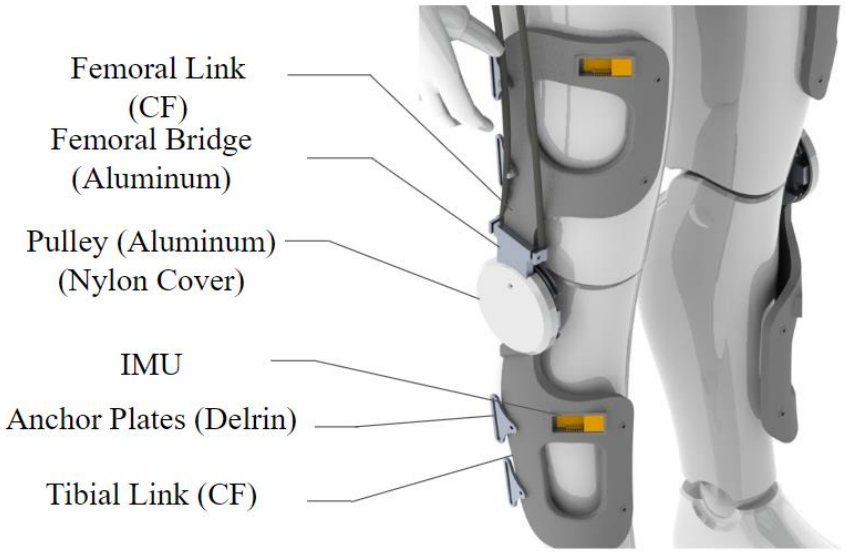

Figure 13. The new design of the lower limb section.

The new femoral and tibial links are 3D-printed and reinforced with a carbon fiber reinforced polymer (CFRP) outer layer to increase strength. This maintains an excellent strength-to-weight ratio. Additionally, the pulley system, which is still made of aluminum, underwent further redesign in order to optimize for minimal volume at the knee joint - as shown in Figure 14. As discussed later, FEA was used in order to both reinforce weak points and reduce the volume of overdesigned areas. The system also contains built-in bowden cable housing clamps, allowing for easy attachment of the cable housing. Delrin (acetal resin) anchor plates are used to attach straps. Additionally, the pulley is designed with stopping edges such that it is impossible for the leg to extend past a human range of motion.

Figure 14. Minimization of profile at the knee joint.

Major improvements were also made to the back brace, as shown in Figure 15. The back brace is also reinforced with CFRP and wraps around the user's waist for a more stable attachment. The placement of the new pancake motors is far more form-fitting than the previous design. The motor pulley has a diameter equal to one-eighth the diameter of the knee pulley, allowing for a 1:8 gear ratio. As a result, it must allow for the cable to wrap around up to three times, as the motor pulley must rotate approximately 960 degrees to attain a rotation of 120 degrees about the knee joint.

Figure 15. The redesigned back brace.

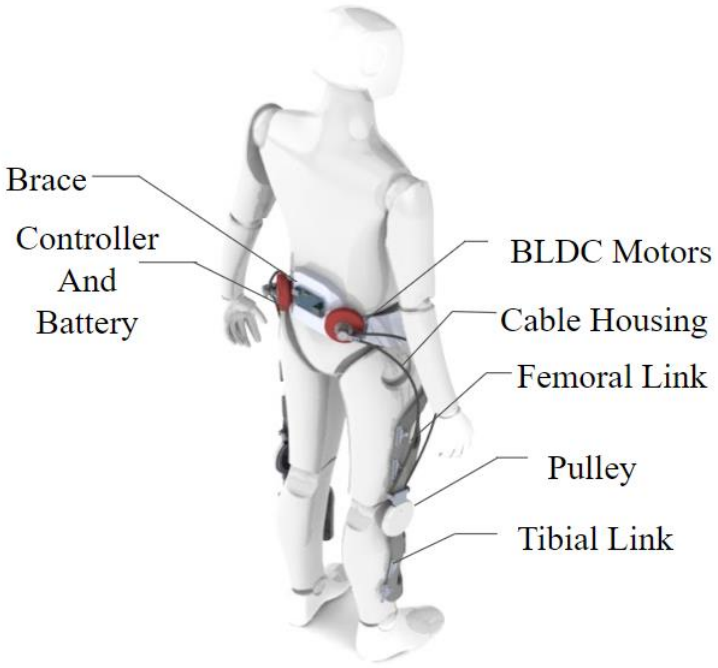

Figure 16. Annotated isometric view of the overall design.

Shown in Figure 16 is an annotated view of the overall design. It is extremely form-fitting, lightweight (estimated to weigh less than 7 pounds), and comfortable.

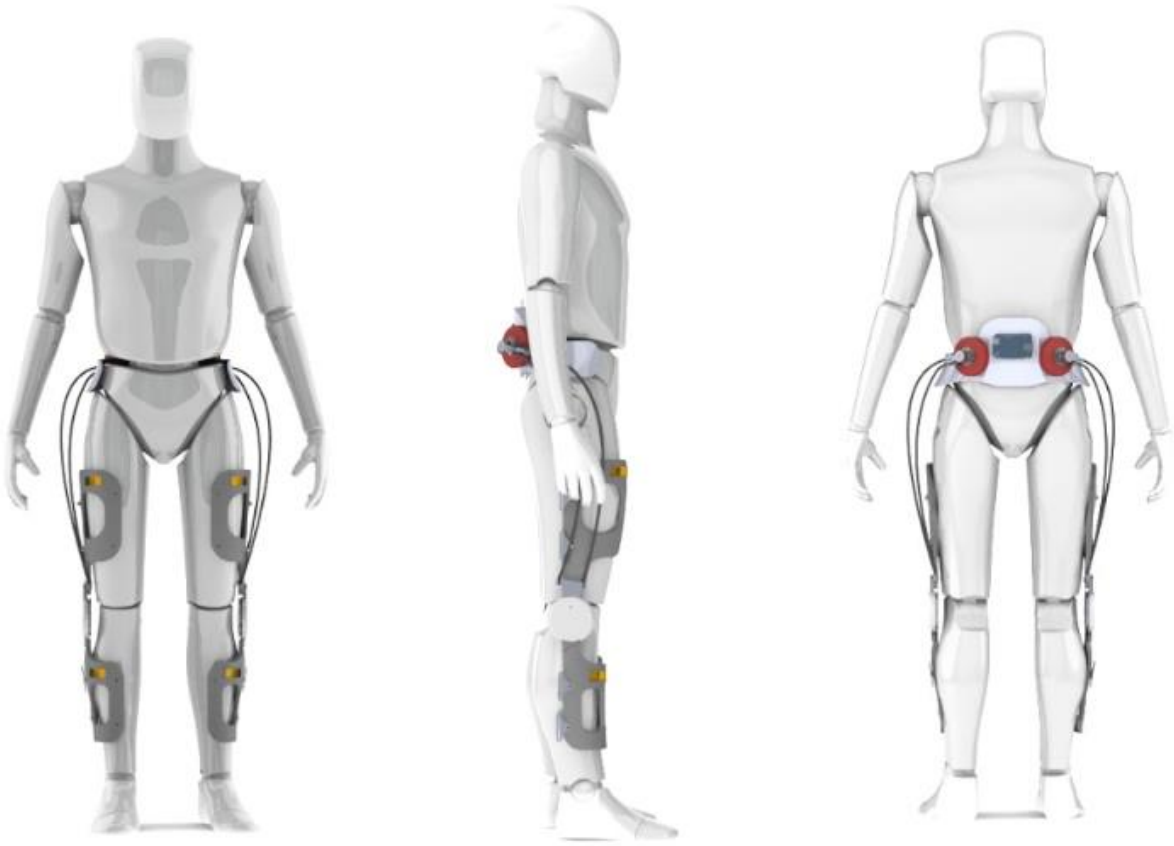

Figure 17. Front, back and side views of the rendered design.

3. Analysis

3.1. Mesh Generation and Boundary Conditions

Finite Element Analysis (FEA) was performed to determine if the load-bearing aluminum components of the exoskeleton were structurally stable. This was necessary because of the high loads present in our design which are caused by the high torque of the motor. FEA was only performed on the aluminum parts because it is an isotropic material that is easy to simulate in SolidWorks. The femoral and tibial links were made by wrapping carbon fiber around 3D printed filament. This would be extremely difficult to replicate in SolidWorks because carbon fiber is an orthotropic material, and thus we decided we would do physical testing instead of FEA for those components.

The torque requirements for the exoskeleton were such that the maximum tension in our cable was 220 lbf. This force is applied via a cable to the cable mount. In this new design rather than using cable stoppers to prevent the cable from slipping through the cable mount as in the previous semester, we simply tied the cable in a knot. When the motor begins to rotate, the cable goes into tension and exerts a load perpendicular to the face of the cable mount. The cable mount then transfers this load to the knee pulley since it is attached mechanically to the cable mount by bolts.

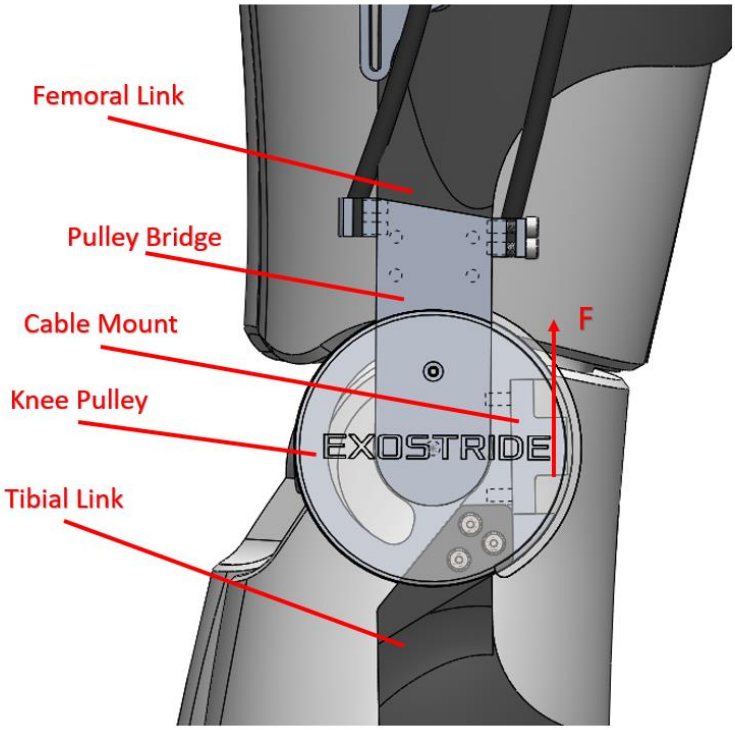

Figure 18. Mechanical components of the lower portion of the exoskeleton. The load being applied by the cable onto the cable mount is also shown, and is labeled F. The cables in the model end at the pulley bridge; however, in the real world they wrap around the pulley.

This load from the cable pulley is then transferred to the tibial link and to the pulley bridge. As mentioned previously since the tibial link will be evaluated with physical testing, we did not perform FEA on this part. Since we are interested in the maximum loading condition we decided to apply the load in a position different from the one shown above. In the diagram shown below, the person would be in a squatting position with legs bent at 90 degrees and the force applied to the cable mount would be perpendicular to the long side of the pulley bridge. This would induce a bending moment on the pulley bridge, rather than just having it be in compression as it would be in the diagram above.

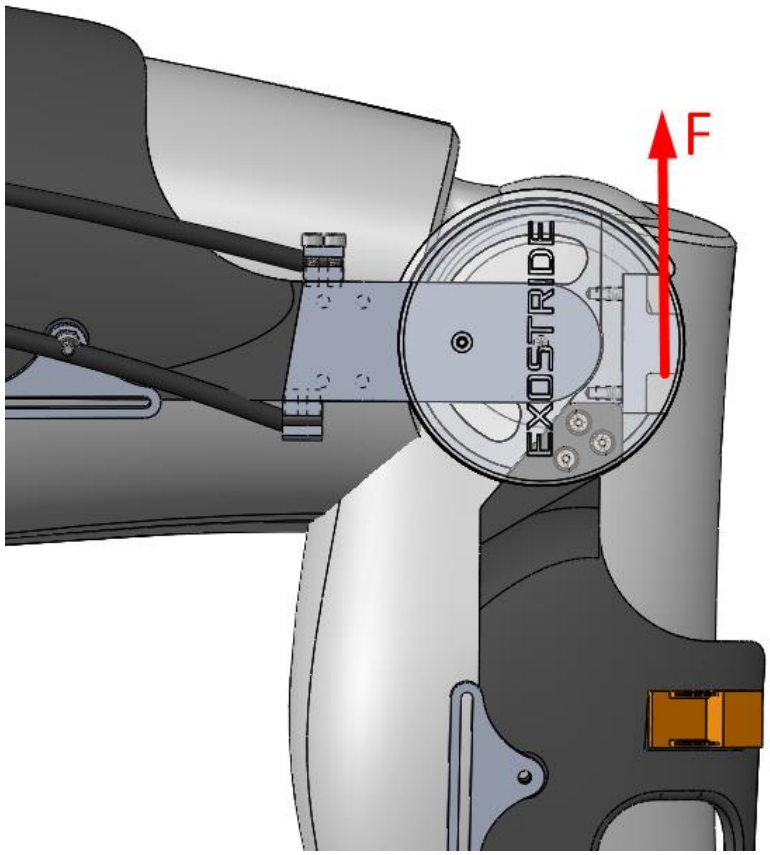

Figure 19. Force F being applied to the exoskeleton while it is in a 90 degree squatting position.

In addition to this we also had to perform an analysis on some of the aluminum components of the motor-cable system shown in the diagram below. The motor is an outrunner, which means that the outside of the motor rotates. This causes the motor pulley to rotate as well since it is rigidly attached to the motor via bolts. The cable bridge is connected to the back brace via bolts as well. The purpose of the cable bridge is to support to cables and feed them into the motor pulley, which wrap around it. The cable bridge and pulley are attached to each other via the connecter, and between the connector and the pulley bridge there is a bearing. As the motor rotates, load is transferred to the motor pulley, however this rotational force is not transmitted anywhere other than to the cable because a bearing cannot transmit a moment. The cable also exerts a force on the cable housing and the motor pulley because it is in tension due to the motor rotating. The connector is not a load bearing component because its only purpose is to provide an attachment point for the bearing, so FEA was not performed on it.

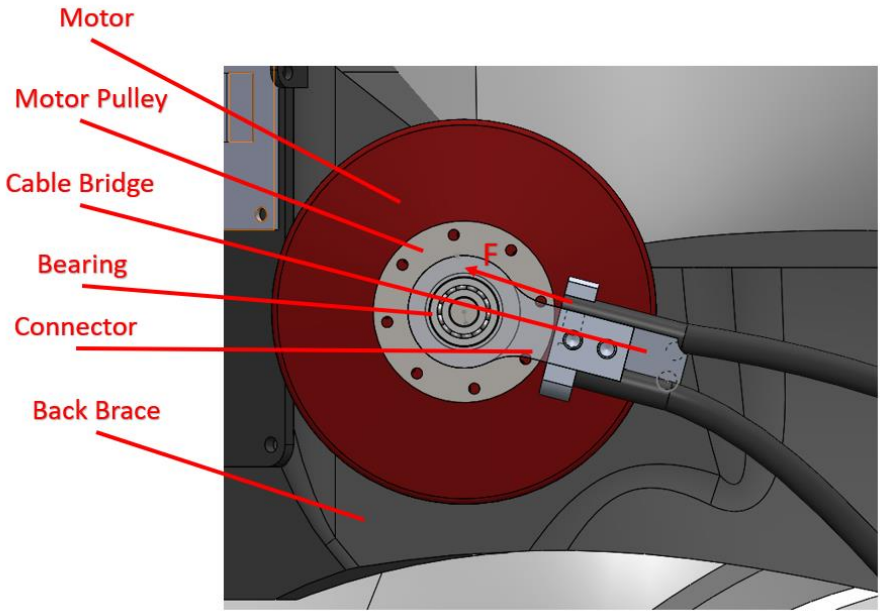

Figure 20. Diagram of the components motor-cable system.

The boundary condition for the cable mount was as follows. A fixed restraint was applied at the surface that contacted the pulley. This was assuming the bolts were properly tensioned and that slip between the surfaces did not occur. It is important to note that when two components are fastened by bolts, it is the friction between the two surfaces that holds them together and not the actual shaft of the bolt. Any two components connected with bolts/screws had their fixed restraint boundary conditions applied using this method. A force of 220 lbf was applied at the location where the stopper contacts the pulley. The boundary conditions are shown below.

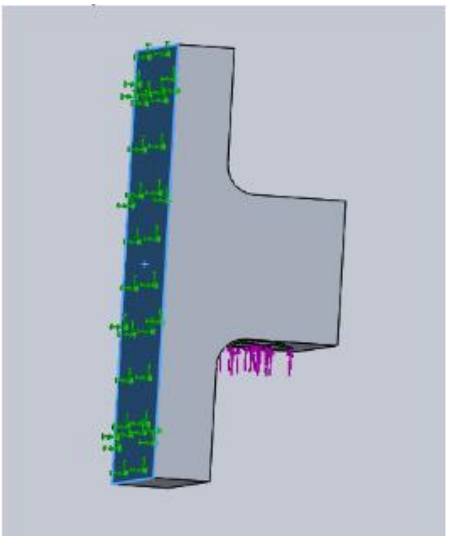

Figure 21. Boundary conditions applied to the cable mount.

To save time during the simulations, the first trial run was always done using global mesh refinement. These results were not recorded, but were used to determine the areas of maximum stress. The mesh was then locally refined in these areas. Since this was done for each FEA, so to avoid redundancy, the global mesh won't be shown for subsequent components. The areas of local refinement were where the maximum stress was found. The two meshes used are shown below.

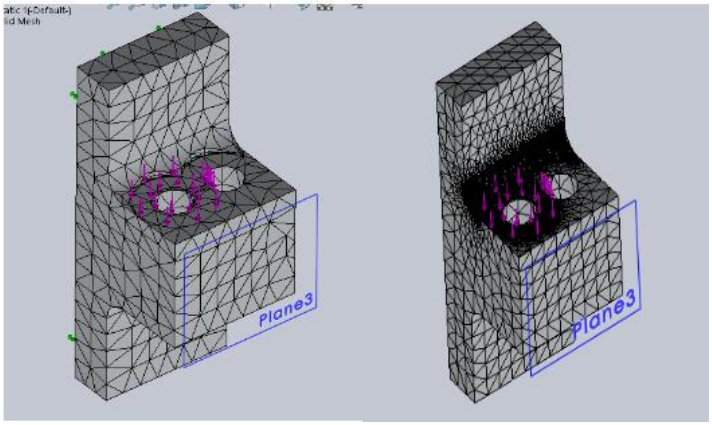

Figure 22. The mesh on the left is the global mesh used for the trial run, and the mesh on the right is the final mesh used.

The boundary conditions and mesh for the knee pulley are shown in the picture below. A fixed restraint is applied to the surface where it is connected to the tibial link. This is because under maximum loading, the lower leg would not be moving. A hinge restraint is placed where

the pulley is connected to the bearing. A remote load (220 lbf) using rigid links is used to apply the load to the pulley. The location of this remote load is the location where the cable is exerting a force on the cable mount.

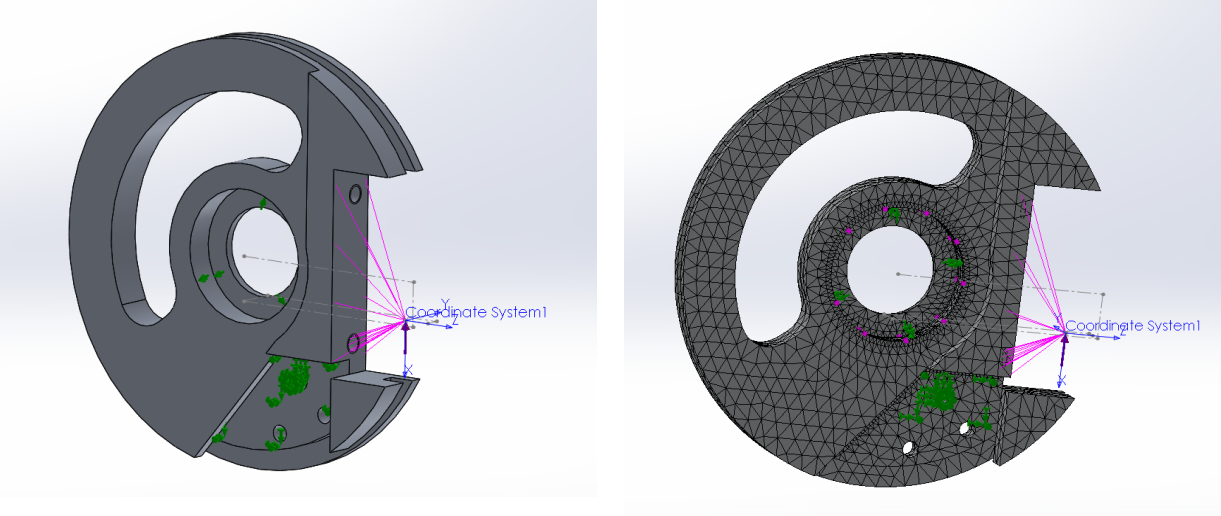

Figure 23. Boundary conditions (left), and mesh (right).

The boundary conditions for the pulley bridge are shown below. An evenly distributed load of 220 lbf is applied to one half of the surface that is in contact with the bearing. This load is caused by the knee pulley pressing into the femoral bridge when the exoskeleton is at 90 degrees. There is a fixed restraint applied where the pulley is in contact with the femoral link. This would be the case for maximum loading.

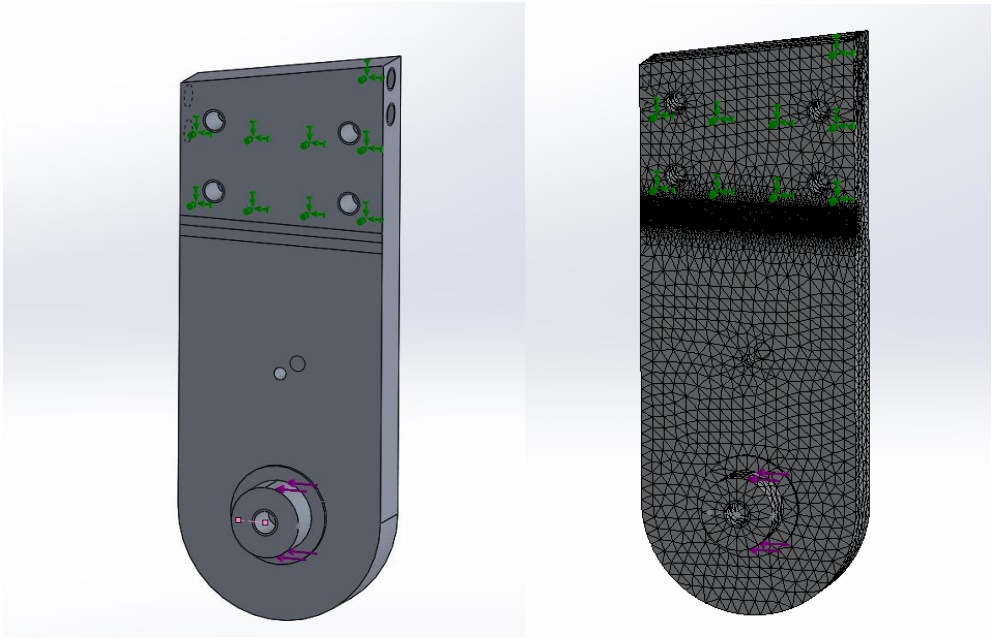

Figure 24. Boundary conditions applied to the pulley bridge (left), and mesh (right).

The boundary conditions and mesh for the motor pulley are shown below. When the motor is active, there is tension in the cable which exerts on force on one side of the shaft of the pulley. An evenly distributed load of 220 lbf was applied to one half the face of part of the shaft. A fixed restraint was applied to the part of the motor pulley that was fixed to the motor, and a bearing restraint was applied to the end of the pulley that is in contact with the bearing.

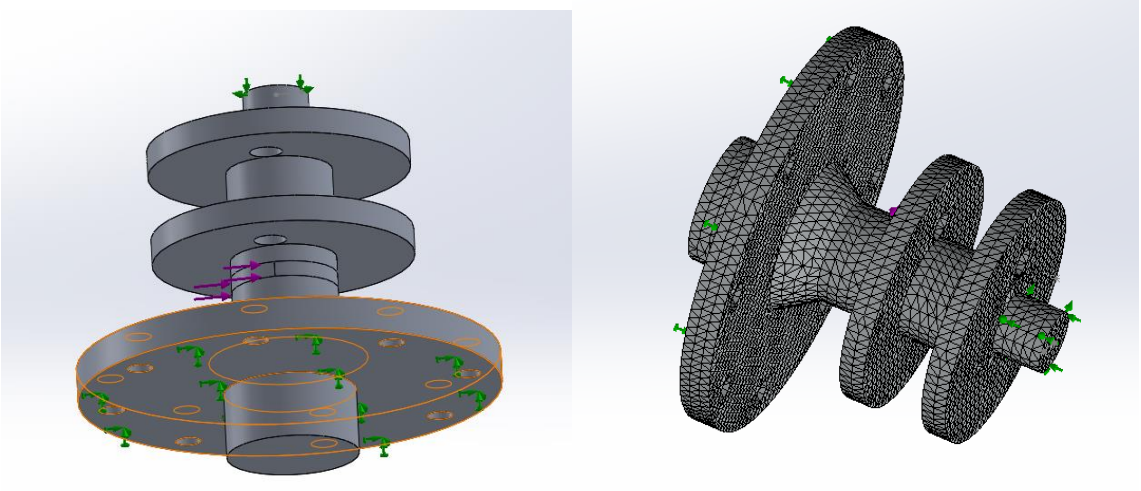

Figure 25. Boundary conditions applied to the motor pulley (left), and mesh (right).

The boundary conditions and meshes for the cable bridge are shown below. The cable has two different sets of boundary conditions due to the asymmetrical nature of its loading. Depending on which way the motor was spinning, the forces would be either acting on the top or bottom of the component. We will call these Case 1 and Case 2. The two common boundary conditions common to both cases are the fix restraints on the faces that are connected to the back brace and to the connector. In Case 1, the force is acting on the bottom of the cable, and a fixed restraint is used to simulate a screw holding the cable housing in place. The force is a distributed force of 220 lbf, which always acts downwards because it is getting pulled towards the knee pulley. In Case 2, the force is now acting downard on the top face of the cable bridge. There is no need for a fixed restraint at the cable housing because no force is exerted on it.

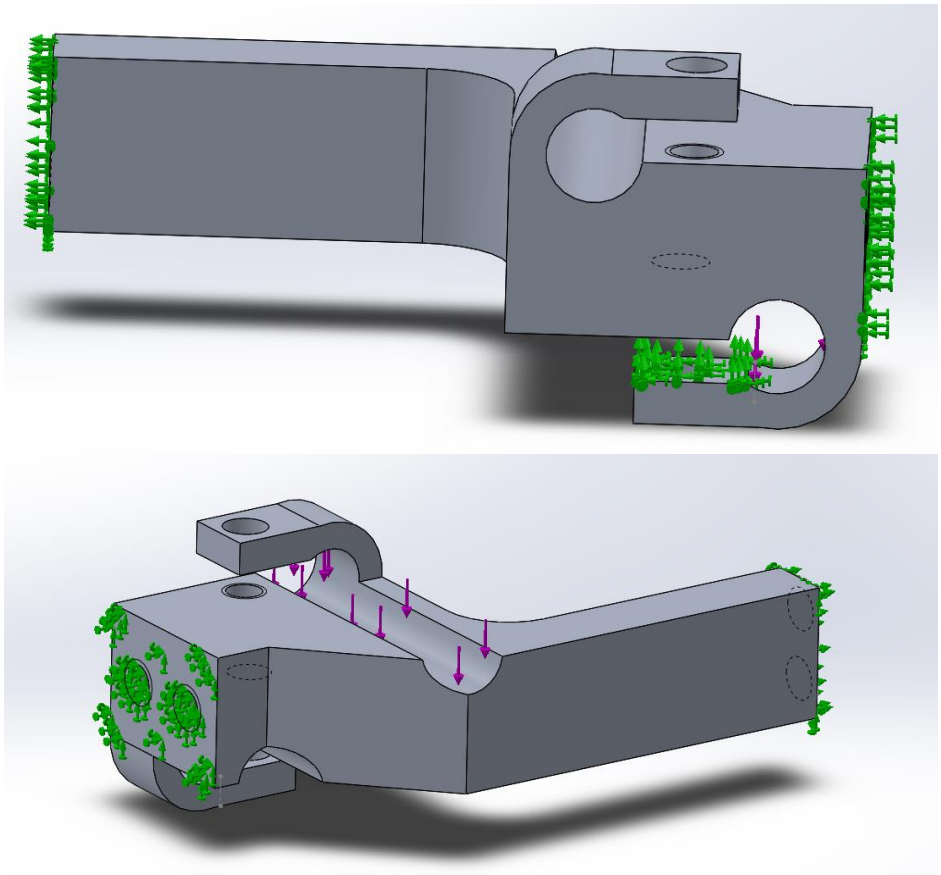

Figure 26. Boundary conditions for Case 1 (top) and for Case 2 (bottom).

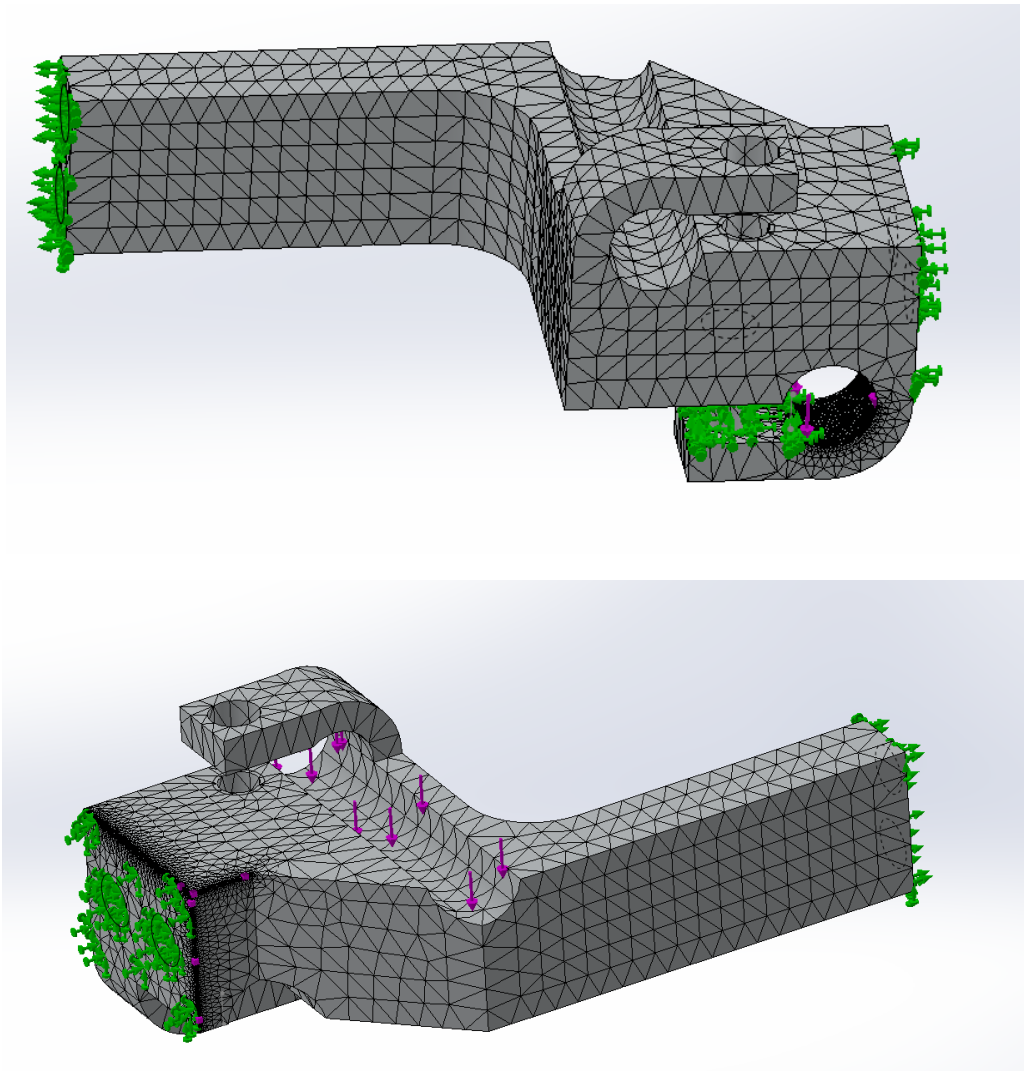

Figure 27. Mesh for Case 1 (top), and mesh for Case 2 (bottom).

3.2. Finite Element Analysis Results

The aluminum was 6061-T6 aluminum which has a yield strength of 270 MPa. Since deflection was not a major concern, our failure criteria was based on yield strength since it is good practice to not have your components permanently deform. The yield strength of our material was 270 MPa, which meant that with a factor of safety of 2, our design strength was 135 MPa. This means that stresses in our components should not exceed this value.

The displacement plot of the cable mount revealed that the surface on which the force was applied was displaced the most, and the surface furthest away which is fixed to the pulley was displaced the least. Since this is what was expected in the real world, the boundary conditions were determined to be accurate. A displacement plot is shown below.

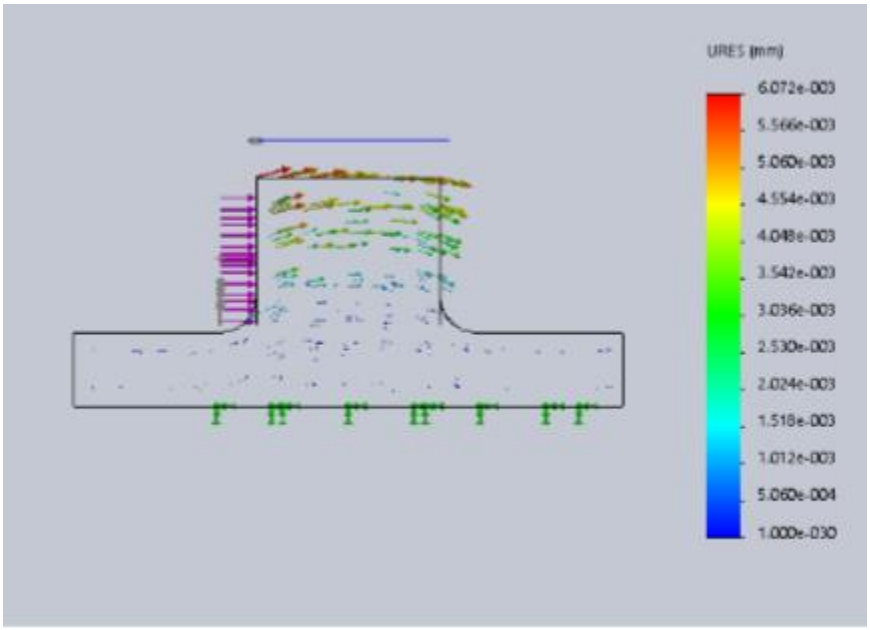

Figure 28. Displacement plot for the cable mount.

When the FEA study on the cable mount was performed, it was found that there was a stress singularity due to a 90-degree edge in the location shown below. Stress singularities discussed in this report were identified by testing to see if the stress in those elements blew up to infinity.

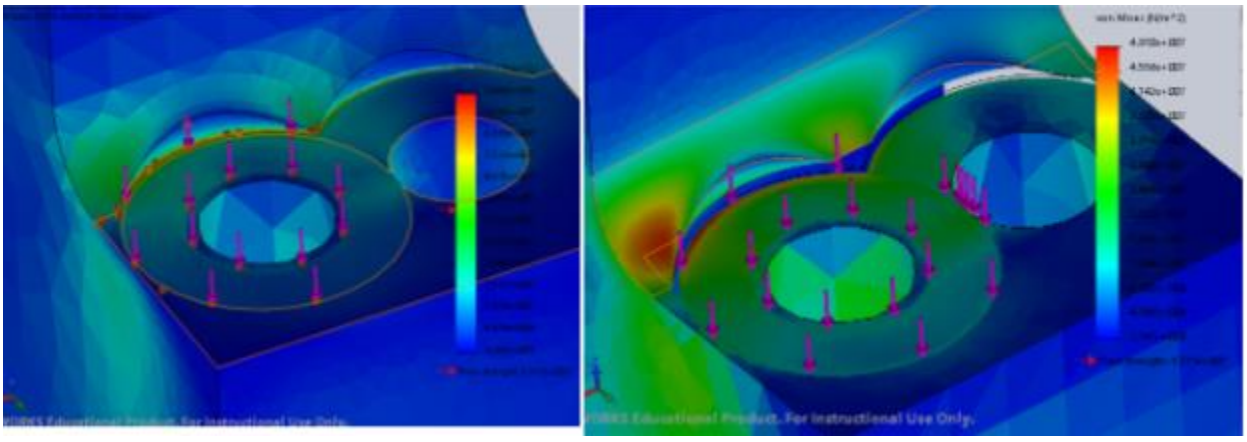

Figure 29. Von Mises stress plot of cable mount. On the left is the stress plot with the stress singularity. The right shows the location of maximum stress after the region with the stress singularity was removed from the plot.

The convergence plot showed the maximum stress converged to a value of 70 MPa, and is shown below. A split line was used to create a surface on which the results were omitted to ignore the stress singularity (shown in Figure 29 above (right)).

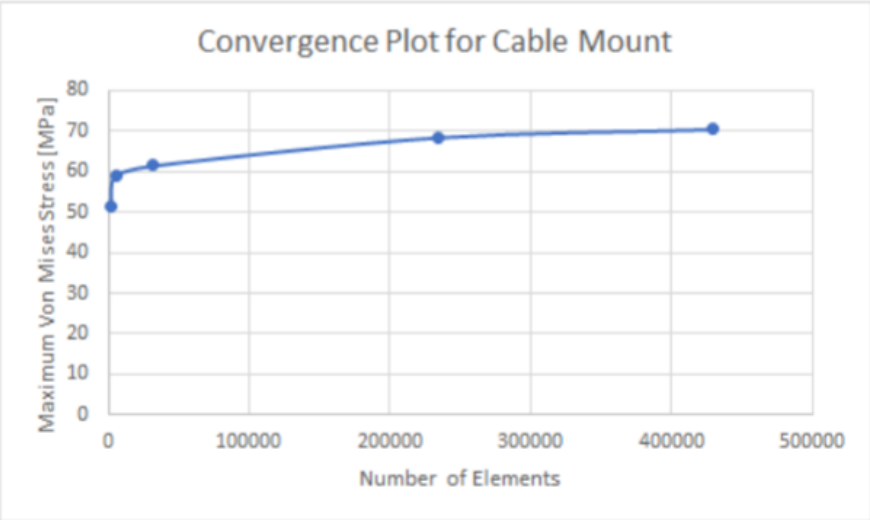

Figure 30. Maximum von Mises stress versus the number of elements in the mesh for the FEA study on the cable mount.

The displacement plot shows vectors which show that the pulley is being deformed in a rotation-like pattern. The minimum displacement is at the fixed restraints as we would expect. The maximum stress occurred near where the bearing was located and converged without any stress singularities to a value of 84 MPa which was below our design strength of 135 MPa. Below are the displacement, stress and convergence plots for the knee pulley.

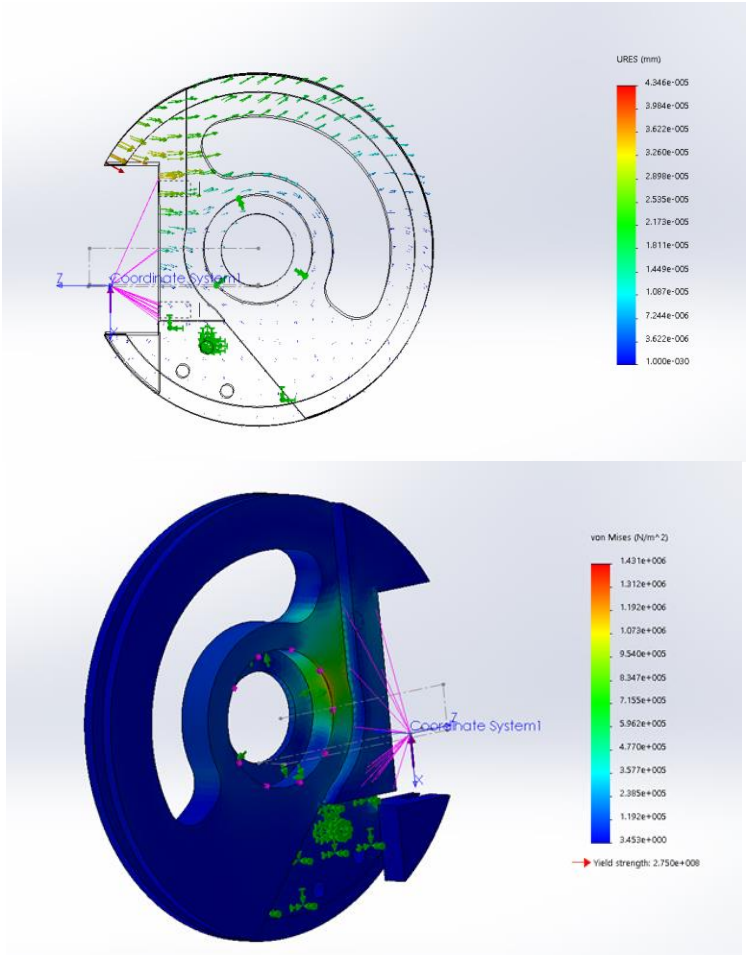

Figure 31. Displacement plot of the knee pulley (top), and the stress plot of the knee pulley (bottom).

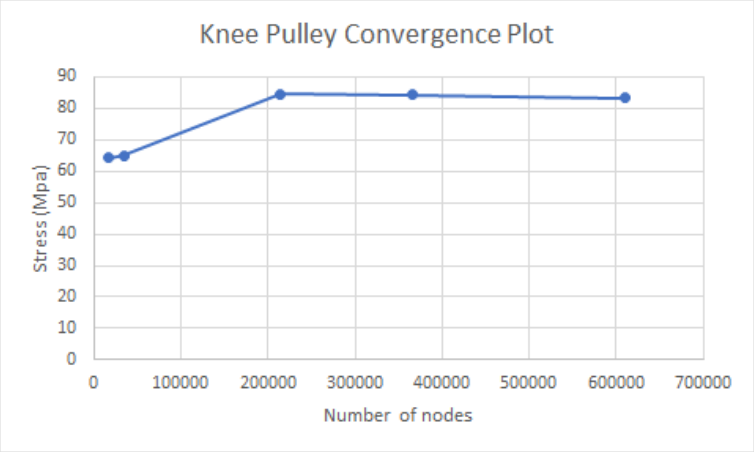

Figure 32. Maximum von Mises stress versus the number of elements in the mesh for the FEA study on the knee pulley.

The displacement plot for the pulley bridge shows that there was minimum displacement near the fix restraint, and that it increased with distance. The displacement was in the same direction as the force and appeared to be slightly rotating around the fixed restraint which is what we would expect in bending. This led us to believe our boundary conditions were accurate. The stress analysis revealed stress was highest near the fixed restraint which we also expected. Due to stress singularities at a fixed restraint, our technique to get meaningful readings was to sample the stress readings a short distance away (using the probing tool) from the fixed restraints where stress singularities fade away. The maximum stress was 36.68 MPa which was below our design strength. Below are the displacement, stress, and convergence plots for the pulley bridge.

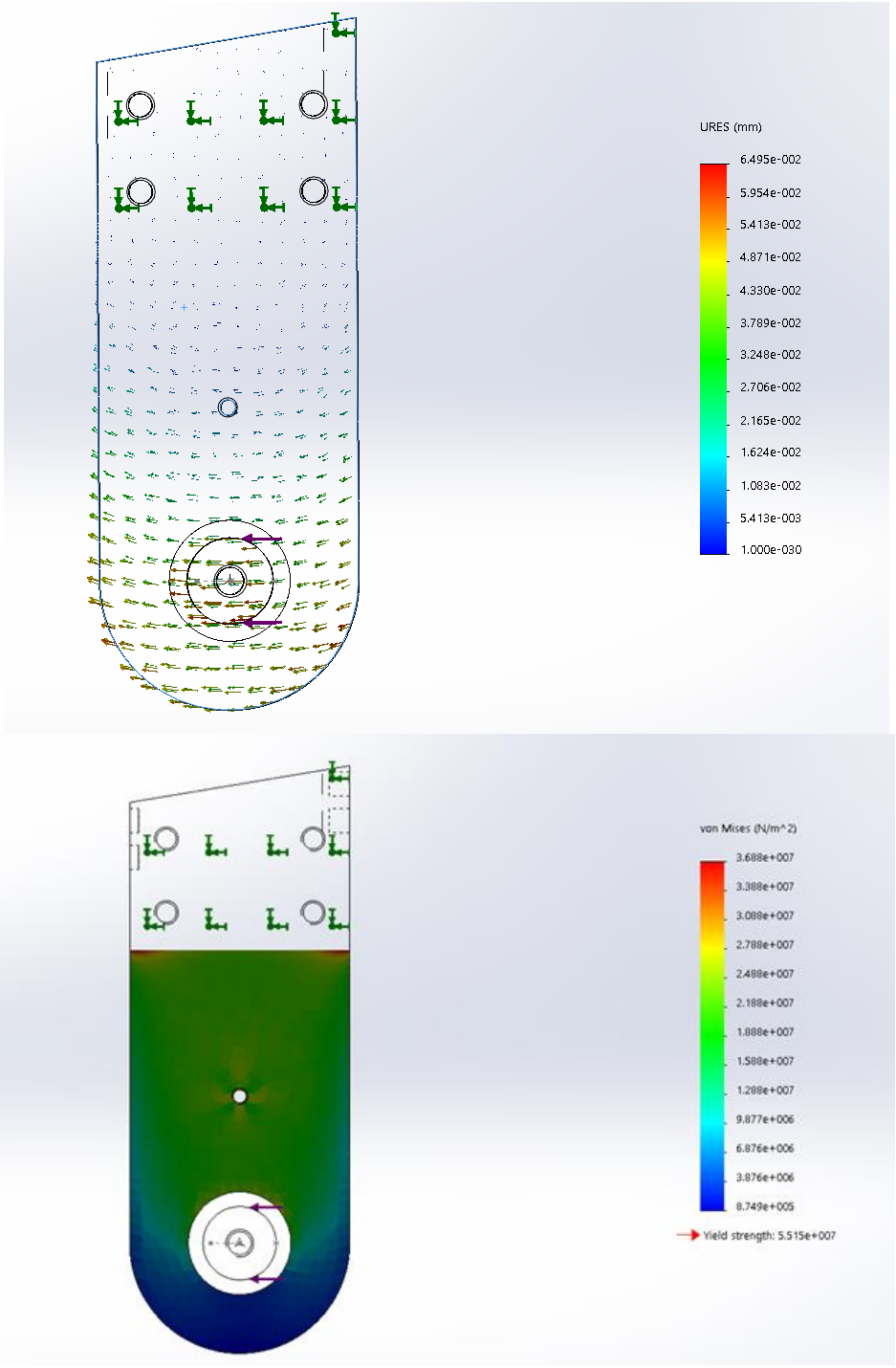

Figure 33. Displacement plot of the pulley bridge (top), and stress plot of the pulley bridge (bottom).

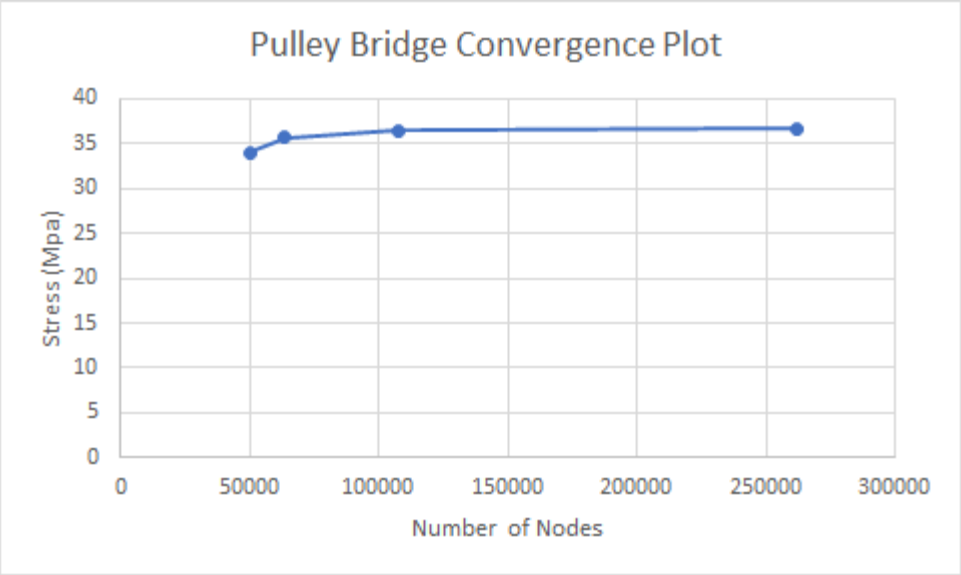

Figure 34. Maximum von Mises stress versus the number of elements in the mesh for the FEA study on the pulley bridge.

The displacement plot for the motor pulley showed that the maximum displacement was at the middle of the pulley and in the direction of the force. This was expected since this is what happens when a beam that is fixed on both sides is loaded in the middle. This is similar to our pulley since our pulley is fixed on both of its ends. Based on this we decided that our boundary conditions were accurate. The stress plot revealed that the maximum stress was at the location where the force was being applied. At first we thought this was a stress singularity; however, after sampling elements a short distance away, the stress still converged and was the maximum stress. The stress converged to a value 9.65 MPa which is well below our design strength. Below are the displacement, stress, and convergence plots for the pulley bridge.

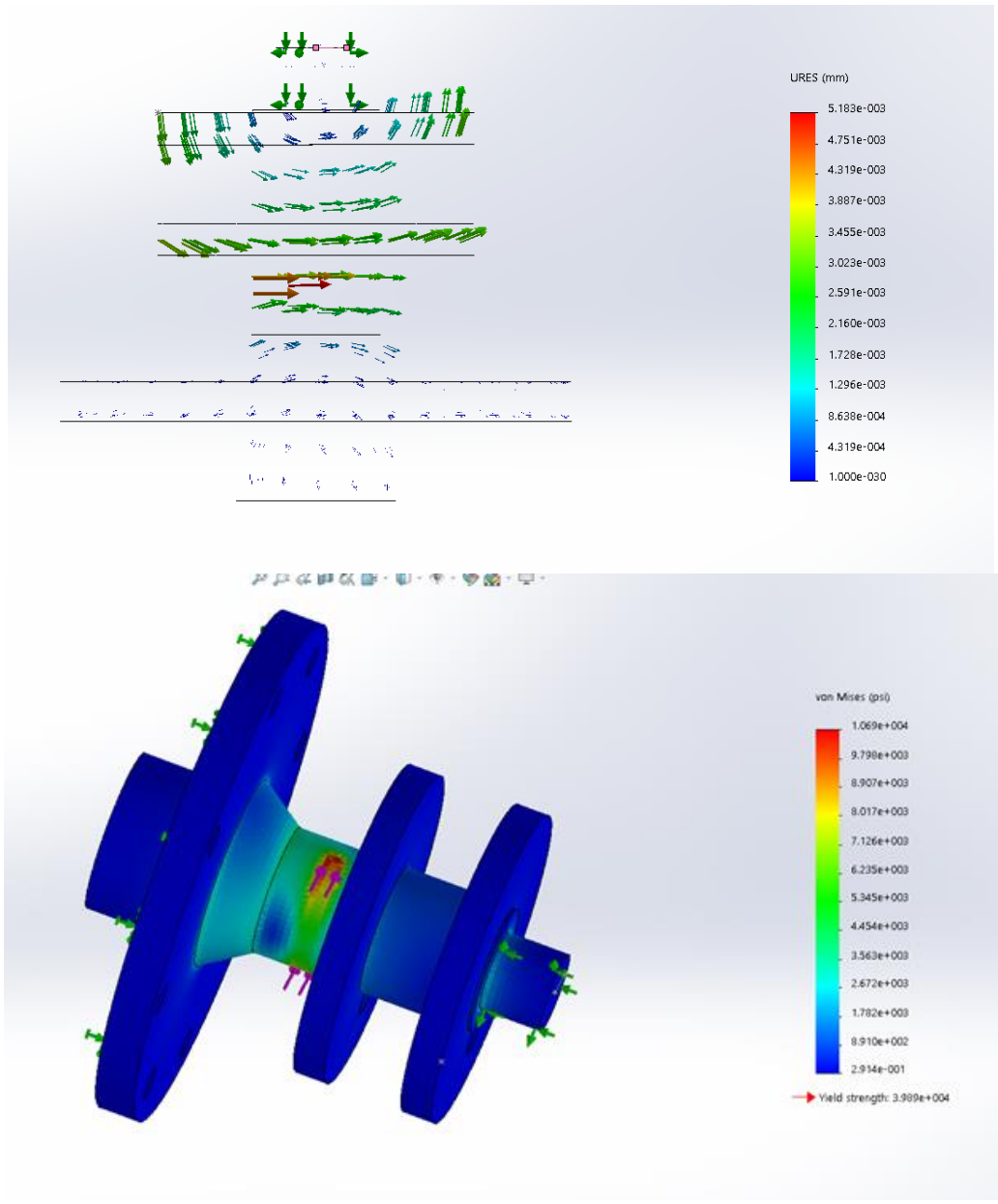

Figure 35. Displacement plot of the motor pulley (top), and stress plot of the motor pulley (bottom).

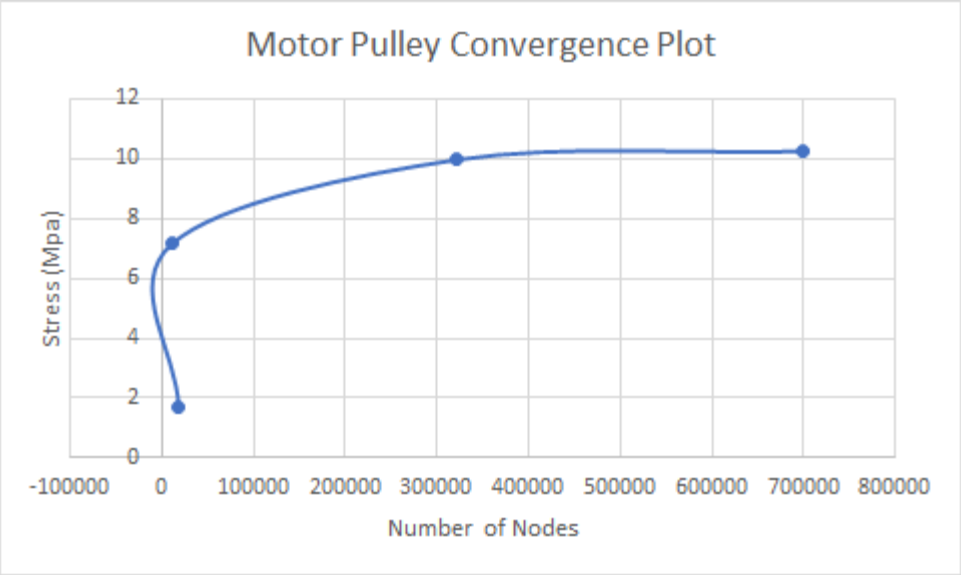

Figure 36. Maximum von Mises stress versus the number of elements in the mesh for the FEA study on the motor pulley.

The displacement plot for the cable bridge (Case 2) shows that the maximum displacement occurred at the cable housing in the direction of the force which is what we expected to happen, with little displacement occurring anywhere else. The maximum stress also in the cable housing was 65 MPa which is below our design strength. To avoid the stress singularity at the border of our fixed displacement we sampled the stress elements a short distance away from the border. Below are plots of displacement, stress, and convergence.

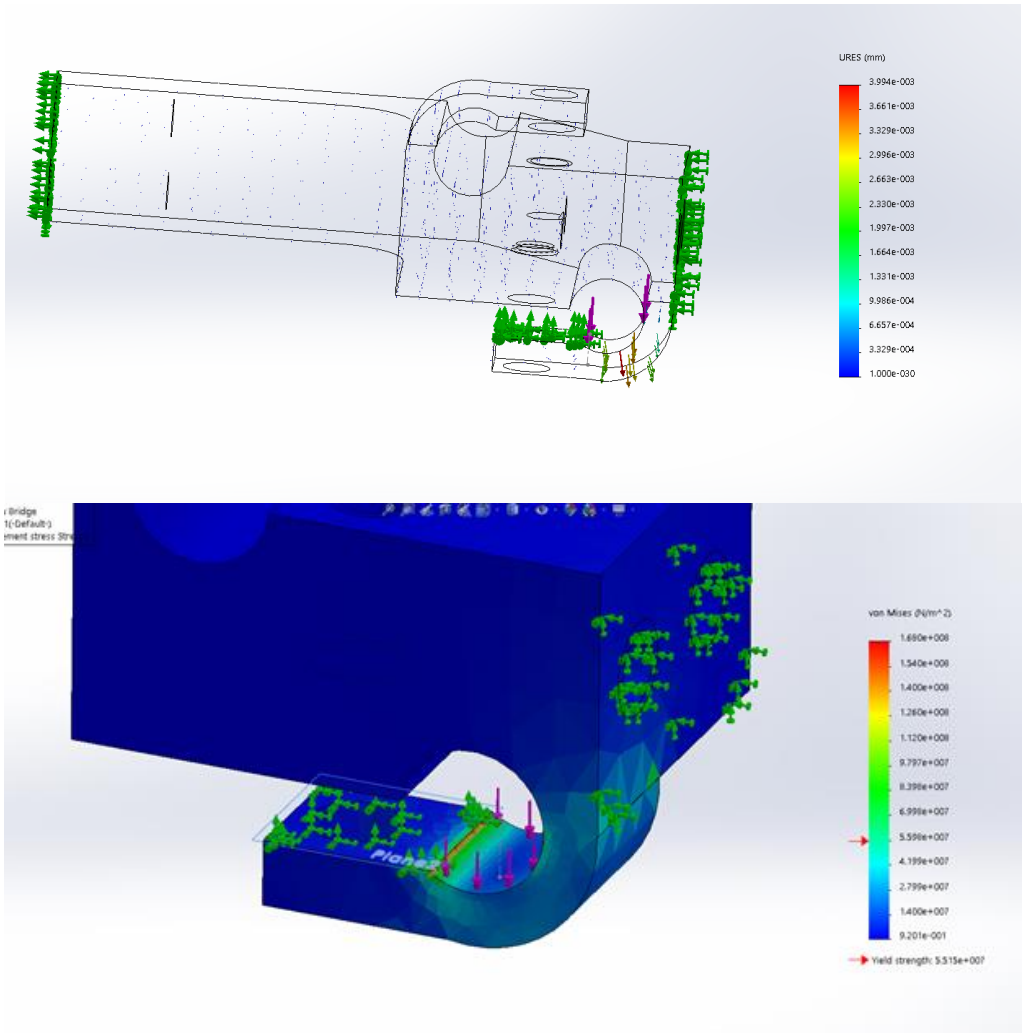

Figure 37. Displacement plot of the cable bridge for Case 2 (top), and stress plot of the cable bridge for Case 2 (bottom).

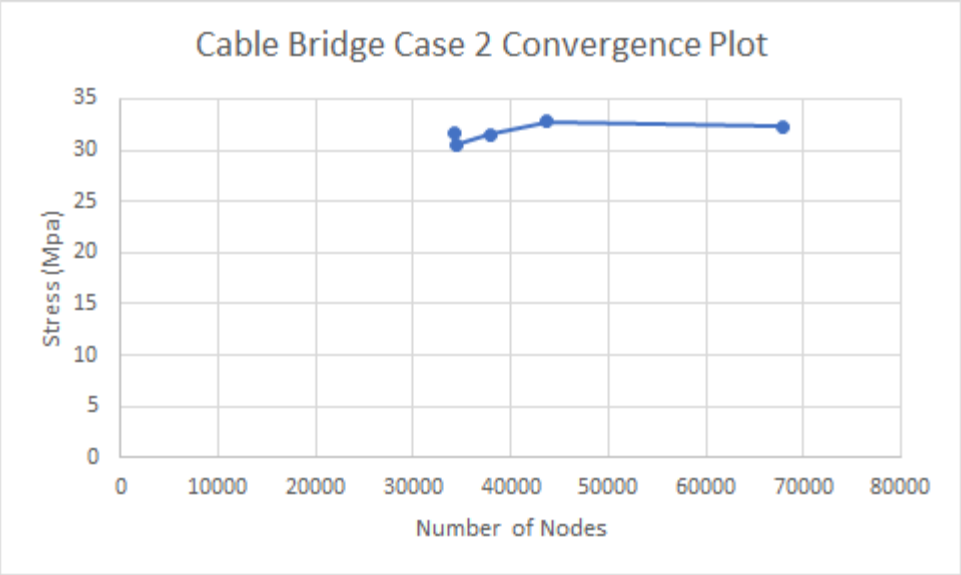

Figure 38. Maximum von Mises stress versus the number of elements in the mesh for the FEA study on the cable bridge (Case 2).

The displacement plot showed the most displacement happening at the location where the load was applied and in the same direction of the load. The stress analysis showed that the maximum stress was on the left side of the cable housing which was connected to the connector and converged to a value of 32.32 MPa.

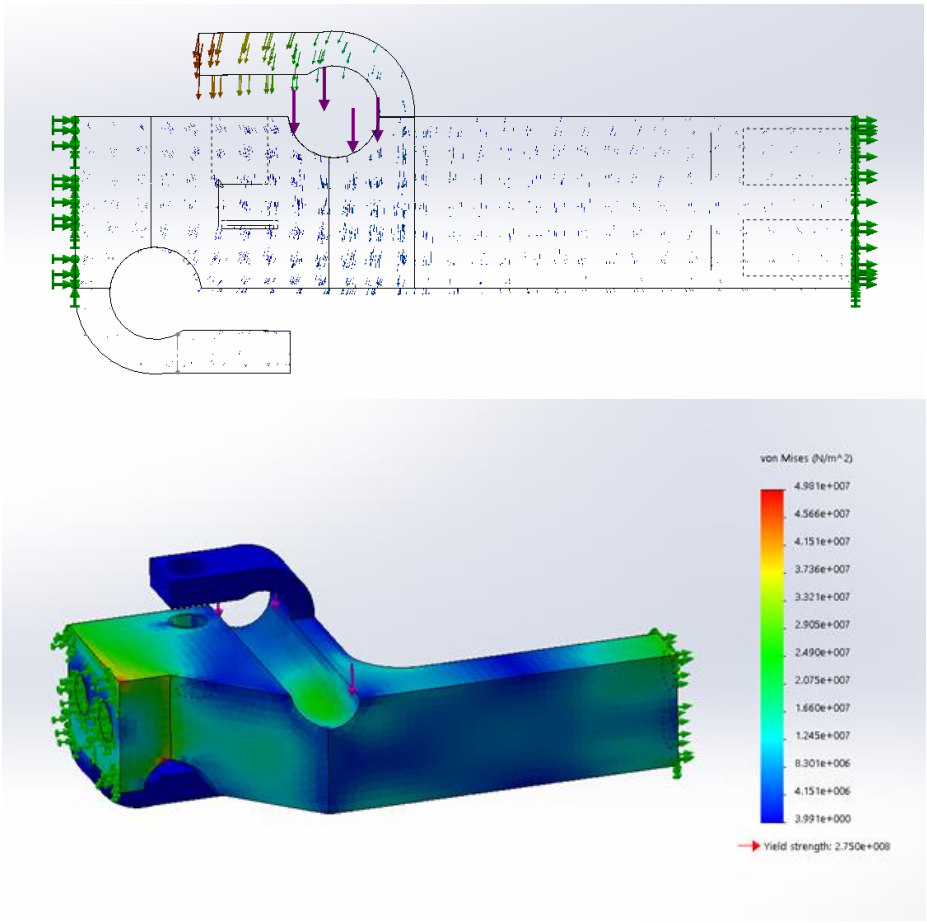

Figure 39. Displacement plot of the cable bridge for Case 1 (top), and stress plot of the cable bridge for Case 1 (bottom).

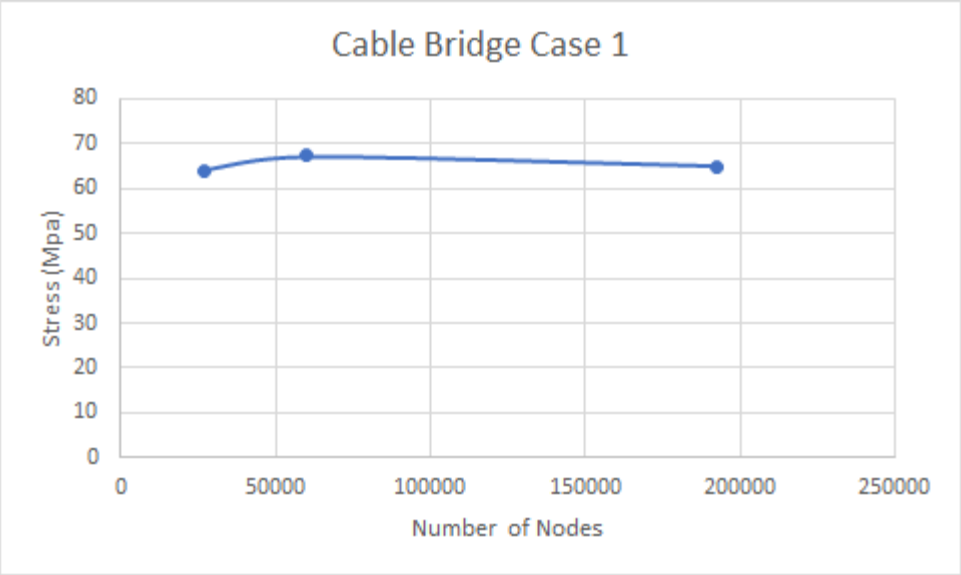

Figure 40. Maximum von Mises stress versus the number of elements in the mesh for the FEA study on the cable bridge (Case 1).

Based on these results we concluded that we could safely CNC our aluminum parts without the risk of them yielding. We also realized that the cable bridge, motor pulley, and pulley bridge were overdesigned. The maximum yield strength in those components wasn't even half of our design strength, which means we could have room to reduce the weight of our components which is a huge factor in exoskeletons. The less weight, the less power is needed, and the more efficiently a person can walk.

3. Manufacturing

Utilizing 3D printers in the Biomechatronics and Intelligent Robotics Lab, the CCNY Robotics Lab, and the Zahn Innovation Center, we printed out the two members and the back brace with ABS and PLA. A 25% infill (the percentage of material to empty space inside the piece) was used in order to minimize weight. Additionally, the ABS/PLA do not support the load, so strength is not a major concern.

Shown in Figure 41 is the second prototype built. This prototype was entirely 3D-printed. Both its dimensions and function were tested to great success. Following its completion and evaluation, we moved onto the carbon fiber lay up phase.

Figure 41. Testing leg exoskeleton prototype on human.

Originally a vacuum bag was to be used in the carbon fiber laying process, as it would ensure equal pressure along the surface area and thus create an even layer of coating, but the pump we bought was revealed to be broken and did not have a high enough pressure rating.

Figure 42. 3D-printed parts being prepared for carbon fiber laying.

Before we started the actual carbon fiber laying, we performed a few trial runs with some previously 3D-printed pieces in order to get a feel for it and to get practice.

Everything was prepared beforehand. The 3D printed piece was sanded down to give it a rough surface, and the surface on which we were going to lay the carbon fiber was given a layer

of wax to prevent the resin from sticking. A piece of the carbon fiber weave was cut out based on the side of the piece we were covering.

Next, a coat of generic adhesive was applied to the surface of the 3D printed piece. The cut of carbon fiber was then adhered to the PLA/ABS as carefully as possible, to avoid messing up the weave pattern. The resin and hardener were then mixed together in a 1:2 ratio and stirred until the exothermic reaction occurred. Gloves and a filtered mask were required at this stage as fumes and heat are produced during the reaction.

Following this reaction, the resin mixture was applied on top of the weave-covered piece. Several layers were applied to make sure the entire carbon fiber surface had an even coating. Afterwards, a roller was used to smooth out any air pockets that may have formed.

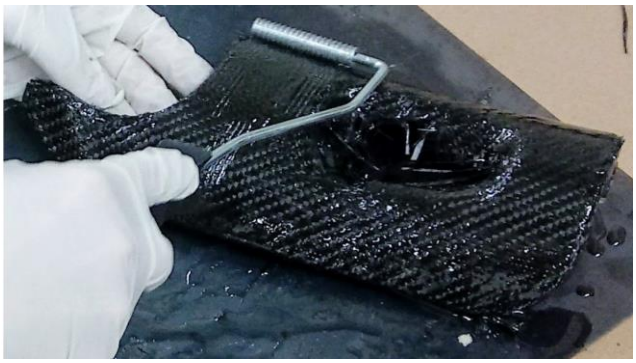

Figure 43. Smoothing out air pockets.

The carbon fiber layered piece is then left to dry for 8+ hours. We let it dry overnight which is sufficient time. Because it is difficult to wrap the carbon fiber weave around an entire object without messing up the pattern, we layered the 3D printed pieces one side at a time. As such, we had to do this process twice for each piece, once for each side.

Figure 44. A nearly completed femoral link.

The pieces were then trimmed with a Dremel to cut off any strands of carbon fiber sticking out, and wet sanded to give it that traditional, glossy carbon fiber look. The last step was marking the locations for the holes with a punch and then drilling the specified holes.

Because we were in the Zahn competition, we had access to their facilities, such as their personal CNC machine. Using our Zahn funding, we hired Andres of CNC to mill our aluminum parts. We then drilled and tapped the necessary holes by hand.

For the straps, we bought Velcro straps and cut them to the appropriate size. We outsourced the sewing to a professional seamstress. For the padding, we decided on using adhesive foam, since it was thin yet soft enough to be comfortable. Using Solidworks' built in "Flatten Surface" feature, we were able to determine the pattern needed, which we traced onto the foam and cut out. We would have applied it to each of the members, but decided to do so last minute in case we needed access to the back side for things such as the screws.

We decided to use Vectran, a manufactured polyester fiber, for the cable due to its high tensile strength. Its main disadvantage is that it frays easily, but we avoided that by keeping it covered in a steel cable housing. Both were purchased in spools and we had to cut them down to length ourselves.

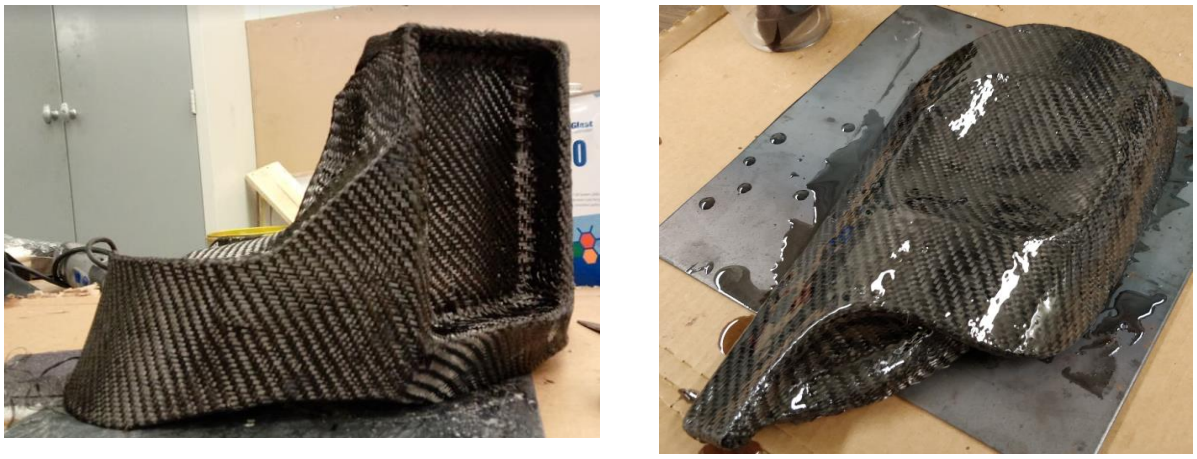

Figure 45. The back brace and femoral links being manufactured.

Figure 46. The back brace and femoral link immediately after the completion of the carbon fiber lay up.

We assembled the final prototype after all of the pieces were manufactured and refined until everything fit snugly. Shown in Figure 47 is Michael wearing the leg exoskeleton to make sure the pulley joint aligned with his knee and that all the straps were able to hold the exoskeleton in place without slipping. After we were satisfied with the physical components and how smoothly they moved and interacted with each other, we attached the electrical components.

Figure 47. Testing the completed exoskeleton.

5. Electronics

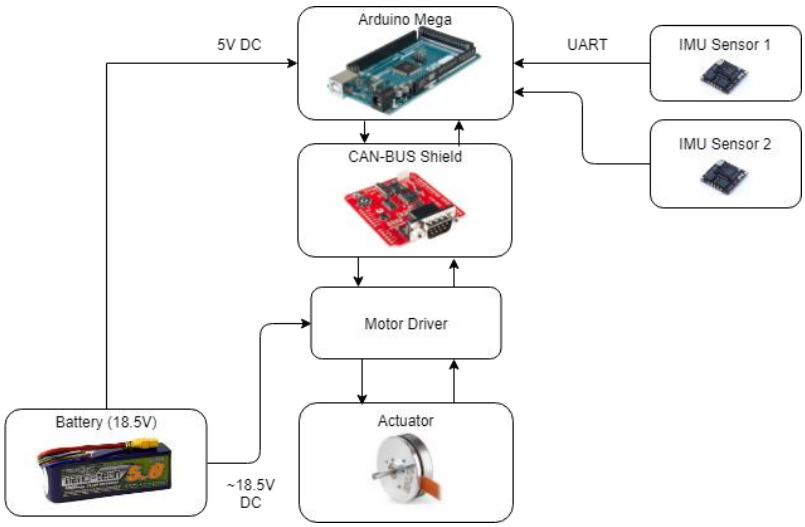

Figure 48. Block diagram of the electrical system.

Shown in Figure 48 is the electrical system for the final prototype. An Arduino Mega serves as the microcontroller. Connected directly to it is an Arduino CAN bus shield used to interface with the motor driver. The high torque brushless DC motor is rated for up to 42 Volts, but for this exoskeleton, an 18.5 V battery is sufficient, as increasing the voltage mainly increases the RPM (current correlates more directly with torque), and high RPM is not necessary for this application. The motor has a built-in encoder, allowing for position and velocity control. Two IMU (inertial measurement unit) sensors are used in order to detect the relative angle of the tibial and femoral links with respect to each other, as well as their angles with respect to the ground plane. Shown in Figure 49 is the completed electrical system.

The system was coded for two main control schemes to be tested. In the first scheme, the leg actuation mirrors the movement of the user's leg movement by following the angle provided by the IMUs. In the second scheme, the actuator remains unpowered until a squatting motion is detected by the IMUs. Once the user reaches a full squat and remains still, the actuator kicks in to help the user stand up again.

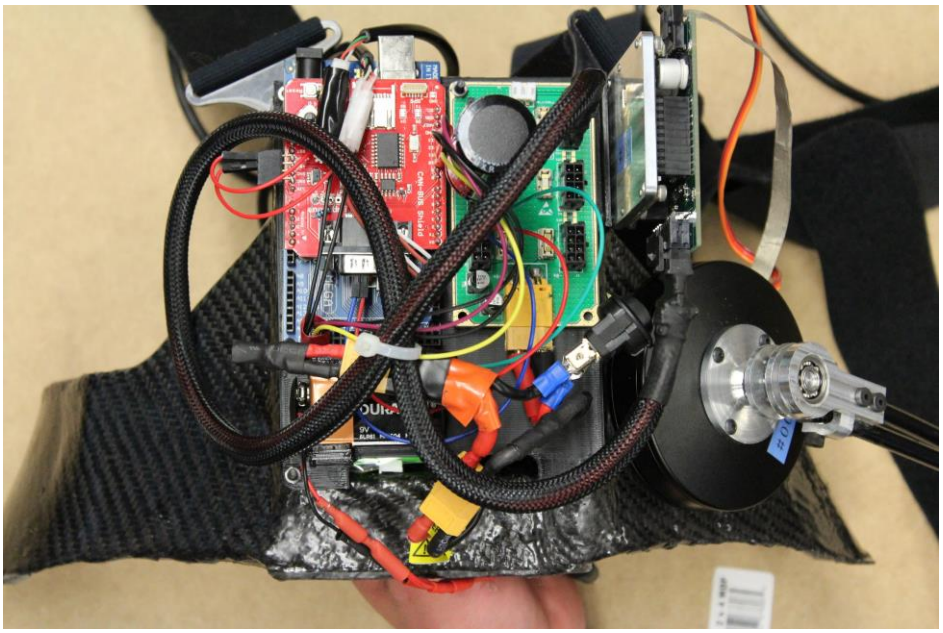

Figure 49. The completed electrical system.

The control system involved using two HI129 Inertial Measurement Units (IMU) for each leg. As none of us have previous experience designing control systems with exoskeletons, we decided to implement a simple control system. To simplify our model, we assumed a 1 degree of freedom system with rotation about the knee joint. The control system we decided on was position control. Based off the angle between the upper and lower legs, the motor would be actuated by a certain number of degrees. The primary basis of our control system was having the motor respond to the change in leg angle. The leg angle is the angle between the upper and lower legs. This was determined by placing an IMU on the upper and lower part of the leg. These IMU's use a combination of accelerometer, gyroscope, and magnetometer data as well as an onboard processor to perform data fusion, to accurately determine the IMU's angle relative to the ground. By determining the difference between the angles that the IMUs were tilted by, and since we know their starting positions relative to each other (calibrated when the person is standing upright), we can determine the leg angle using the following equation:

$$\theta_{leg} = 180° - \theta_1 + \theta_2$$

The placement of the IMUs is shown in the figure below. The origins of the two XY coordinate systems are where the IMUs would be placed. They are to be rigidly attached to the tibial and femoral links. The angle theta is the angle of tilt relative to the ground, and omega is the angular velocity of the leg. The angular velocity could be used for future work to try to

predict user intentive. The velocity can be calculated by subtracting two consecutive IMU measurements and dividing that by the time that passed between the measurements.

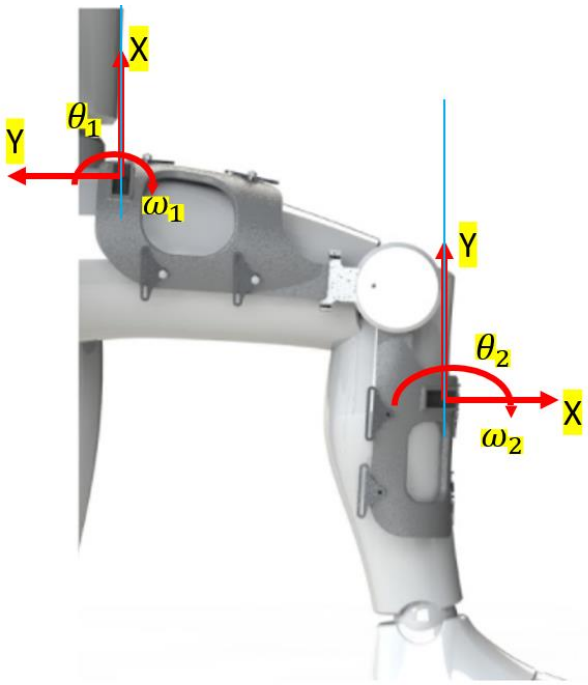

Figure 50. Locations of the IMUs on the exoskeleton.

A block diagram of our control system is shown below. The two IMUs give out a reading from which the leg angle is calculated. Since our IMUs had a lot of noise, we created a median filter to filter out the noise. The median filter works by saving the IMU readings into a 7 element buffer and taking the median value as the true value of the leg angle. 7 elements were chosen because it was found that the IMUs did not produce three random spikes in the leg angle in a row. Although this made the response time slower, it was the only way to eliminate high peaks. A median filter with less elements could be used, however it would require better IMUs. After the leg angle passes through the median filter it is fed to the controller (Arduino). The control algorithm tells the motor to rotate by 1/8th the amount of the degrees the leg angle changed by. This is because the ratio of the motor pulley to the knee pulley is 1:8.

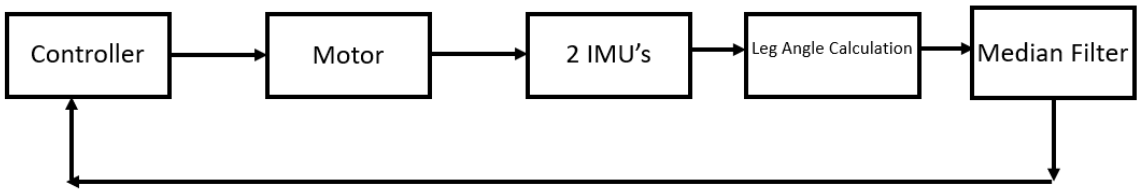

Figure 51. A block diagram representing our control system.

6. Results and Discussion

6.1. Ergonomics

Figure 52. Professor Sadegh wearing the exoskeleton while lifting a box.

The completed exoskeleton was demonstrated on a variety of different people of different sizes. Due to its flexible nature, the device fits comfortably on anyone within roughly 5’4” to 6’2” tall. The strap system, which allows for comfort, requires about 30 seconds to attach or detach.

Feedback was overwhelmingly positive in terms of comfort. However, weight was still an issue, with some testers asking to reduce the weight further. Compared to other exoskeletons on the market, this device is extremely lightweight, which shows just how important the weight of an exoskeleton matters when bringing it to the mass market.

6.2. Control System

We tested this control system by attaching the IMUs to Michael as shown in Figure 53. As Michael moved his leg, the IMUs detect the change in angle, and this information was used to calculate the leg angle which was passed through a median filter. This was then sent to the controller which made the motor rotate the exoskeleton that was attached to the mannequin. The control system was a success. The mannequin followed the leg movements that Michael was performing.

We did not have time to implement velocity control to predict user intentions, however this was still a very important stepping stone in our design process. This simple control system demonstrated that it was possible to accurately measure the leg angle and control it using a motor without the use of heavy torque sensors. Another way that we could predict user intent is through the use of force sensitive resistors which we experimented with. Knee exoskeletons are by nature very complicated, and there is a lot to be done in future works which will be discussed in a later section.

Figure 53. Testing of the control system using a mannequin.

6.3. Biomechanics

In order to determine how much torque to provide to the knee and to better visualize how squatting works from a biomechanics and energy standpoint, it was recommended we do a biomechanical analysis. There are several program suites that can analyze human biomechanics but Prof. Hao Su recommended B.O.B. and Anybody. B.O.B. is an add-in for MATLAB that allows the user to analyze a human model during any coded motion and determine the torques, moments, and energy expenditure involved in that motion. Anybody is a much more involved program, and allows for manipulation of parameters, such as weighted objects. In order to analyze data in either of these programs, the motion must first be coded. There are two ways to do this: either through hardcoding, or using a motion capture device. With the guidance of Prof. Su, we opted for the motion capture device.

The motion capture device we used is called Perception Neuron. Perception Neuron is a collection of 32 IMUs and a central hub. The IMUs are worn all over the human body, from head to toes, and communicate amongst each other. Through the included Axis Neuron software, one can record the location and angle of all of the IMUs for a given period of time. This information is output as a 3d model, but the raw IMU data can also be accessed. For this project, we chose to record the movement of a human lifting a box. The output can be seen in Figure 54.

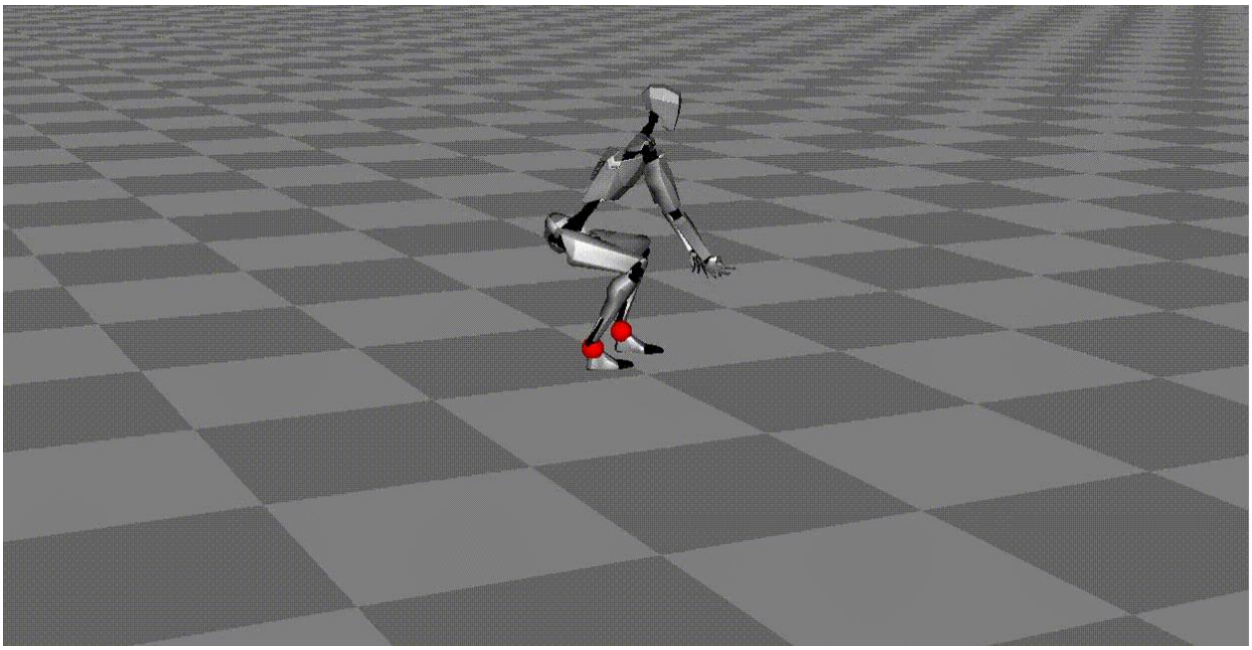

Figure 54. 3D model generated by Perception Neuron IMUs

Once the raw data for lifting was obtained, we first chose to import it into B.O.B. Through B.O.B. we are able to select several parameters, including joint moments, joint torques, joint angles, energy expenditure, load forces etc. We are primarily interested in the torque around

the knee, so we chose that parameter. The results can be seen in Figure 55. The simulation predicted an estimated 70 Nm of torque around the right knee during the lifting motion that we recorded using the motion capture software. This ensured that our selected application of 40Nm is appropriate. It should be noted that B.O.B. is a rather rudimentary program, and we could not find any documentation regarding its accuracy.

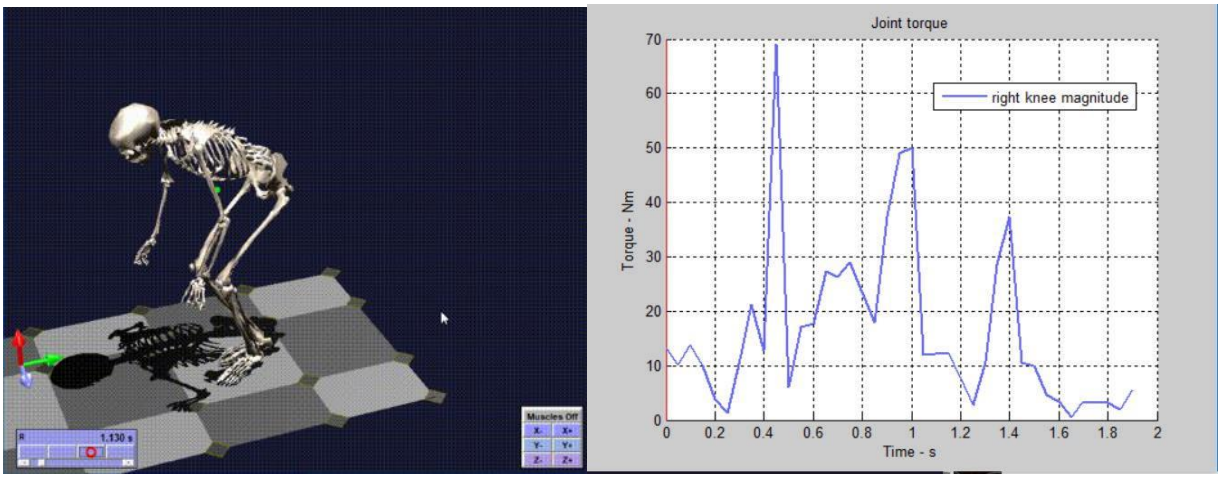

Figure 55. Data obtained from B.O.B.

We wanted to create a scalable model so that we could not only simulate the assistance of an exoskeleton, but vary the torque provided by the exoskeleton to choose an optimal torque. B.O.B. does not have this capability, so we chose to use Anybody. We also wanted to confirm our B.O.B. results of our raw IMU analysis with a seperate program to verify the results. We ran into several problems with this program, however. Anybody is a much more difficult program to use than B.O.B. because B.O.B. is simply an add-in to MATLAB, a program we are very familiar with. Anybody uses its own code language and unique library so learning to code with it has been an arduous task. We know that this task is possible to do, as Prof. Hao Su has created a scalable exoskeleton model with Anybody in the past; however, it did not incorporate motion capture data, but rather a mathematically ideal lift that was hardcoded into the program. Even with the assistance of several of Prof. Su's graduate students, we could not properly incorporate the motion capture data into Anybody. We are still working on this, however, as this is a feature which would lend much insight into the scalability of our exoskeleton.

7. Future Works

There are several more improvements that could be made. Our goal was to program the exoskeleton to detect the intention of the wearer, and only apply torque when it has determined that the user is lifting something. This prevents the exoskeleton from constantly interfering with

basic human movement. Though we are close to successfully implementing this, we have not as yet, and this is the obvious immediate next step.

There are also further weight reductions that could have been made. The electronics we used are generally large, bulky and heavy. If more money was available, we could have bought electronics that are lighter and more compact. We also could layer more carbon fiber and remove PLA to reduce the weight of the exoskeleton while maintaining structural integrity. A cover for the electronics also needs to be implemented, as currently the wires could easily be snagged in the environment. Comfortable padding also needs to be implemented, as well as a more efficient strapping system. The simple velcro straps that are currently being used tend to slide around the human leg while being strapped. Perhaps implementing a sleeve could alleviate this.

8. Conclusion

Over the course of the 2017-2018 academic year, we were able to research, design, and manufacture a robust and functional prototype for a knee exoskeleton. Our design has been shown to be relatively lightweight, comfortable and form-fitting. The control system has been successfully shown to work, and it is expected to produce 40 Newton-meters of force based on mathematical analyses and physical testing. Current models typically produce 20-30 Newton-meters of force, which is considered ideal by industry standards, showing that our design is a cut above the rest. The device is now in its final testing and programming phases and is already capable of predicting and assist with the user's movement. In order to reach a market-ready product, further iterations of implementation, testing, and revision must be done, but with each passing trial our knee exoskeleton is nearer to becoming a real product.

For more information about the progress of our project, please visit www.exostride.com.

References

1. Bureau of Labor Statistics. Nonfatal occupational injuries and illnesses requiring days away from work. Washington, DC: US Department of Labor; 2010. [Accessed September 19, 2012]. News Release USDL-11-1612, November 9, 2011. Available at: http://www.bls.gov/news.release/archives/osh2_11092011.pdf.

2. Chen, Z., Chakrabarty, S., Levine, R. S., Aliyu, M. H., Ding, T., & Jackson, L. L. (2013). Work-Related Knee Injuries Treated in Emergency Departments in the United States. Journal of Occupational and Environmental Medicine / American College of Occupational and Environmental Medicine, 55(9), 1091–1099. http://doi.org/10.1097/JOM.0b013e31829b27bf

3. J. Perry, Gait Analysis : Normal and Pathological Function, Thorofare, NJ: SLACK, 1992.

4. Petrič T., Gams A., Debevec T., Žlajpah L., Babič J., Control approaches for robotic knee exoskeleton and their effects on human motion, Advanced Robotics, 2013, 27, 3, str. 993-1002

5. Pocock, G., Richards, C. and Richards, D. (2013). Human physiology. Oxford: Oxford University Press.

6. S. Hirokawa, “Biomechanics of the knee joint: a critical review,” Critical Reviews in Biomedical Engineering, vol. 21, no. 2, pp. 79–135, 1993.